Università degli Studi di Roma "La Sapienza"

SAPIENZA
UNIVERSITÀ DI ROMA

Dipartimento di Scienze Economiche

Thesis

Applications of Nonlinear Dynamics and Complex Systems Theory to Finance

Submitted in partial fulfilment of the requirements for the degree of Doctor of Philosophy

Advisors
Prof. Carl Chiarella
Prof. Giuseppe Garofalo
Prof. Giulia Rotundo

Author
Alessandro Sansone

Summary

Introduction

In recent years there has been a growing disaffection with the standard economic paradigm of efficient markets and rational expectations. In an efficient market, asset prices are the outcome of the trading of rational agents, in the sense that they forecast the expected price by exploiting all the information available and know that other traders are rational. As pointed out by Fama (1970), if market were not efficient, there would be profit opportunities which would be exploited by the trading of rational agents. This implies that prices must equal the fundamental prices, given by the expected discounted dividend streams, and therefore changes in prices are only caused by changes in the fundamental value. In real markets, however, traders have different information on traded assets and process information differently, therefore the assumption of homogeneous rational traders may not be appropriate. In addition to this, the efficient market hypothesis motivates the use of random walk increments in financial time series modeling: if news about fundamentals are normally distributed, the returns on an asset will be normal as well. However the random walk assumption does not allow the replication of some stylized facts of real financial markets, such as volatility clustering, excess kurtosis, autocorrelation in square and absolute returns, bubbles and crashes. Recently a large number of models that take into account heterogeneity in financial markets has been proposed. The typical agents considered in these model are basically fundamentalists, who believe that prices tend to equal the fundamental value of an asset, and technical traders, who predict future prices by extrapolating past patterns in the time series. Recent contribution to this literature include Beja and Goldman (1980); Day and Huang (1990); Caginalp and Ermentrout (1990, 1991); Chiarella (1992); Sethi (1996); Gaunersdorfer (2000); Gaunersdorfer and Hommes (2005); Chiarella, Dieci and Gardini (2002, 2005); Franke and Sethi (1998); Westerhoff (2003, 2004a, 2004b). Brock (1997), Brock and Hommes (1997, 1998, 2001a) have introduced the important concept of financial markets as adaptive belief systems, in the sense that agents switch prediction rule among different predictors according to a fitness function that depends on the realized profits of a given prediction strategy. Chiarella and He (2001) analyze asset price and wealth dynamics in the framework of Brock and Hommes (1998) and Levy and Levy (1996) without switching among different predictors. Such a model is extended by adding a switching rule between momentum and contrarian strategies by Chiarella and He (2002) in the context of a Walrasian scenario and Chiarella and He (2003) and He (2003) in a market maker scenario. Brock, Hommes and Wagener (2005) analyze the limit evolution of Brock and Hommes (1998) when the strategies are distributed according to a continuous distribution; Thurner, Dockner and Gaunersdorfer (2002) analyze a market composed of a continuum of fundamentalists who show delays in information processing. These models allow for the formation of speculative bubbles, which may be triggered by news about fundamentals and reinforced by technical trading. Because of the presence of nonlinearities according to which different investors interact with one another, these models are capable of generating stable equilibria, periodic, quasi-periodic dynamics and strange attractors.

In Chapter 1 we introduce a model built on that of Thurner, Dockner and Gaunersdorfer (2002), henceforth TDG, which is inspired by the Nosè (1984a,b, 1991) and Hoover (1985) models of thermodynamics and analyzes a financial market in which there are only fundamental investors who trade according to the mispricing of the asset with delays which are uniformly distributed from initial to current time. We generalize TDG by introducing a continuum of technical traders who behave as either trend followers or contrarians and a switching rule between these technical trading rules. As for the fundamentalists, technical traders react with uniformly distributed delays to the information that they receive from the market. We do not assume the existence of a Walrasian auctioneer, but allow for transactions to be made in a condition of disequilibrium by assuming the existence of a market maker who takes an offsetting long or short position so as to clear the market and set the price according to the direction and magnitude of excess demand. We analyze how the interaction of different types of investors with path dependent risk aversions determines the

dynamics and the statistical properties of the system as the proportion of fundamentalists, the growth rate of the fundamental, the speeds of reaction of the market participants and the intensity of switching between technical trading strategies are changed. In particular, the system is characterized by strange attractors that are capable of giving rise to time series of returns featuring stylized facts of real financial markets such as excess kurtosis, volatility clustering and long memory, even in a purely deterministic framework.

Chapter 2 generalize the model by Chiarella, Dieci, Gardini (2006) by introducing a swiching rule between fundamentalists, trend followers and contrarians in a market cleared by a market maker. Differently from most of existing literature, we adopt a flow-based approach and utilize realistic values for the interest rate and the growth rate. In Chapter 3 we generalize the model by assuming both that agents are not fully informed and learn the fundamental price with delays and that there is a share issue proportional to change in wealth that modify the discount rate determining a discount rate much higher than the risk-free rate, contributing in this way to explain both equity premium puzzle and fundamental changes that are not triggered by news.

1. Asset Price Dynamics in a Financial Market with Heterogeneous Trading Strategies and Time Delays

1.1 The model

Let us consider a security continuously traded at price $P(t)$. Assume that this security is in fixed supply, so that the price is only driven by excess demand. Following TDG, let us assume that the excess demand $D(t)$ is a function of the current price and the fundamental value $F(t)$. Differently from the standard financial economic literature, we assume that transactions are not made at equilibrium prices, but that a market maker takes a long position whenever the excess demand is negative and a short position whenever the demand excess is positive so as to clear the market. The market maker adjusts the price in the direction of the excess demand with speed equal to λ^M. The instantaneous rate of return is:

$$\frac{\dot{P}(t)}{P(t)} = \lambda^M D(P(t), F(t)); \lambda^M > 0 \tag{1}$$

the fundamental value is assumed to grows at constant rate *g*, therefore:

$$\frac{\dot{F}(t)}{F(t)} = g \tag{2}$$

The market is composed of an infinite number of investors, who choose among three different investment strategies. Let us assume that a fraction α of investors follows a fundamentalist strategy and a fraction $(1-\alpha)$ follows a technical analysis strategy. The fraction of technical analysts is in turn composed of a fraction β of trend followers and a fraction $(1-\beta)$ of contrarians. Let $D^F(t)$, $D^{TF}(t)$ and $D^C(t)$ be respectively the demands of fundamentalists, trend followers and contrarians rescaled by the proportions of agents who trades according to a given strategy. The excess demand for the security is thus given by:

$$D(t) = \alpha D^F(t) + (1-\alpha)[\beta D^{TF}(t) + (1-\beta) D^C(t)]; \alpha, \beta \in [0,1] \tag{3}$$

Each trader operates with a delay equal to τ, that is, the demand of a particular trader at time t depends on her decision variable at time $t-\tau$. Time delays are uniformly distributed in the interval $[0,t]$.

Fundamentalists react to the differences between price and fundamental value. The total demand of fundamentalists operating with delay τ is:

$$D^{F\tau}(t) = \lambda^{F\tau} \log\left[\frac{F(t-\tau)}{P(t-\tau)}\right]; \lambda^{F\tau} > 0 \tag{4}$$

where $\lambda^{F\tau}$ is a parameter that measures the speed of reaction of fundamentalist traders; we assume that $\lambda^{F\tau} = \lambda^F$ throughout the paper. This demand function implies that the fundamentalists believe

that the price tends to the fundamental value in the long run and reacts to the percentage mispricing of the asset in symmetric way with respect to underpricing and overpricing.[1]
If time delays are uniformly distributed, the market demand of fundamentalists is given by:

$$D^F(t) = \lambda^F \int_0^t \log\left[\frac{F(t-\tau)}{P(t-\tau)}\right] d\tau \,;\, \lambda^F > 0 \tag{5}$$

time differentiation yields:

$$\dot{D}^F(t) = \lambda^F \log\left[\frac{F(t)}{P(t)}\right] ;\, \lambda^F > 0 \,. \tag{6}$$

Following TDG, let us modify equation (6) by introducing the variable $\varsigma(t)^F$ and adding a term $-\varsigma^F(t)D^F(t)$ to the right hand side:[2]

$$\dot{D}^F(t) = \lambda^F \log\left[\frac{F(t)}{P(t)}\right] - \varsigma^F D^F(t) ;\, \lambda^F > 0 \,. \tag{7}$$

According to the sign of ς^F, if there is an excess demand, the term $-\varsigma^F(t)D^F(t)$ either drives it towards zero (if $\varsigma(t)^F$ is positive) or foster it (if $\varsigma(t)^F$ is negative). The variable $\varsigma(t)^F$ may be interpreted as an indicator of the risk that traders bear and their risk aversion (if $\varsigma(t)^F$ is negative, traders become risk-seekers). The dynamics for $\varsigma(t)^F$ are given by:

$$\dot{\varsigma}^F(t) = \delta^F [D^F(t)^2 - V^F] ; \delta^F > 0 \tag{8}$$

where V^F is a variance-controlling factor. Throughout the paper, we will assume that V^F is given. The economic motivation of equation (8) is that, the larger an open position on the asset, the more risk averse the investors become.
Let us consider now the behavior of technical traders. As for the fundamentalists, their time delays are uniformly distributed in the interval $[0,t]$. A trader operating with delay τ utilizes the percentage return that occurred at time $t-\tau$ in a linear prediction rule in order to form an expectation of future returns. The demands of trend followers and contrarians operating with delay τ are respectively:

$$D^{TF\tau}(t) = \lambda^{TF\tau}\left[\frac{\dot{P}(t-\tau)}{P(t-\tau)}\right] ; \lambda^{TF\tau} > 0 \tag{9}$$

$$D^{C\tau}(t) = \lambda^{C\tau}\left[\frac{\dot{P}(t-\tau)}{P(t-\tau)}\right] ; \lambda^{C\tau} < 0 \tag{10}$$

---

[1] TDG utilize $D^{F\tau}(t) = \lambda^F [F(t-\tau) - P(t-\tau)]$ as functional form for the demand of fundamentalists. We rather utilize function (4) because we consider more plausible that fundamentalists react to mispricing in percentage terms. Of course if $F(t-\tau)$ and $P(t-\tau)$ are in logarithm terms, the fundamentalist demand of TDG is equivalent to (4).

[2] TDG introduce the variable ξ, which is linear transformation of $D^F(t)$, and utilize it instead of $D^F(t)$. We will continue to utilize the variable $D^F(t)$ without any loss of generality.

throughout the paper we will assume that $\lambda^{TF\tau} = \lambda^{TF}$ and $\lambda^{C\tau} = \lambda^{C}$. By integrating (9) and (10) with respect to τ and time differentiating we get the time derivatives of the total demands of technical analysts, which are:

$$\dot{D}^{TF}(t) = \lambda^{TF}\left[\frac{\dot{P}(t)}{P(t)}\right]; \lambda^{TF} > 0 \tag{11}$$

$$\dot{D}^{C}(t) = \lambda^{C}\left[\frac{\dot{P}(t)}{P(t)}\right]; \lambda^{C} < 0. \tag{12}$$

As for the fundamentalists, we add now the terms $-\varsigma^{TF}(t)D^{TF}(t)$ and $-\varsigma^{C}(t)D^{C}(t)$ in order to take into account the risk and risk attitude of chartists. Time derivatives of their total demands are therefore:

$$\dot{D}^{TF}(t) = \lambda^{TF}\left[\frac{\dot{P}(t)}{P(t)}\right] - \varsigma^{TF}(t)D^{TF}(t); \lambda^{TF} > 0 \tag{13}$$

$$\dot{D}^{C}(t) = \lambda^{C}\left[\frac{\dot{P}(t)}{P(t)}\right] - \varsigma^{C}(t)D^{C}(t); \lambda^{C} < 0. \tag{14}$$

Following TDG, the dynamics for $\varsigma^{TF}(t)$ and $\varsigma^{C}(t)$ are:

$$\dot{\varsigma}^{TF}(t) = \delta^{TF}[D^{TF}(t)^2 - V^{TF}]; \delta^{TF} \geq 0 \tag{15}$$

$$\dot{\varsigma}^{C}(t) = \delta^{C}[D^{C}(t)^2 - V^{C}]; \delta^{C} \geq 0 \tag{16}$$

We will now consider the fraction α as given, whereas the fraction of trend followers β may be path dependent. In fact β is considered as an endogenous variable because both trend followers and contrarians follow technical analysis strategies and therefore may be likely to switch them if one brings about higher returns. We assume that the more profitable is a strategy, the more investors will choose that strategy. The difference in the absolute return at time *t* between the two strategies is given by $\dot{P}(t)[D^{TF}(t) - D^{C}(t)]$. The use of absolute returns as a measure of evolutionary fitness stems from the absence of wealth in the model, therefore it is not possible to calculate the percentage return of a strategy. Moreover, β must be bounded in the interval $[0,1]$ and we assume that it tends to move towards 0.5 if both the strategies lead to equal profits. These assumptions can be taken into account if we assume this functional form for the time derivative of $\beta(t)$:

$$\dot{\beta}(t) = \cot[\pi\beta(t)] + z\dot{P}(t)\left[D^{TF}(t) - D^{C}(t)\right]; z \geq 0 \tag{17}$$

where the first term keeps the fraction of trend followers bounded in the interval [0,1] and z is a parameter that measure the speed of switching between the technical strategies. The proportion tends to 0.5 if the two strategies are characterized by the same absolute return. Therefore, the dynamics are ruled by the following nine ordinary differential equation system:

$$
\begin{aligned}
&\dot{P}(t) = \lambda^M P(t)\left[\alpha D^F(t) + (1-\alpha)\left[\beta(t) D^{TF}(t) + (1-\beta(t)) D^C(t)\right]\right]; \alpha \in [0,1]; \lambda^M > 0 \\
&\dot{D}^F(t) = \lambda^F \log\left[\frac{F(t)}{P(t)}\right] - \varsigma^F D^F(t); \lambda^F > 0 \\
&\dot{D}^{TF}(t) = \lambda^{TF}\left[\frac{\dot{P}(t)}{P(t)}\right] - \varsigma^{TF}(t) D^{TF}(t); \lambda^{TF} > 0 \\
&\dot{D}^C(t) = \lambda^C\left[\frac{\dot{P}(t)}{P(t)}\right] - \varsigma^C(t) D^C(t); \lambda^C < 0 \\
&\dot{\varsigma}^F(t) = \delta^F\left[D^F(t)^2 - V^F\right]; \delta^F > 0 \\
&\dot{\varsigma}^{TF}(t) = \delta^{TF}\left[D^{TF}(t)^2 - V^{TF}\right]; \delta^{TF} > 0 \\
&\dot{\varsigma}^C(t) = \delta^C\left[D^C(t)^2 - V^C\right]; \delta^C > 0 \\
&\dot{\beta}(t) = \cot[\pi\beta(t)] + z\dot{P}(t)\left[D^{TF}(t) - D^C(t)\right]; z \geq 0 \\
&\dot{F}(t) = gF(t)
\end{aligned}
\tag{18}
$$

If $z=0$ or if the proportion of trend followers and contrarians is taken as a constant, then the system may be made stationary by defining the variable $M(t) \equiv \frac{F(t)}{P(t)}$. In this case *System 18* becomes:

$$
\begin{aligned}
&\dot{D}^F(t) = \lambda^F \log[M(t)] - \varsigma^F D^F(t); \lambda^F > 0 \\
&\dot{D}^{TF}(t) = \lambda^{TF} r - \varsigma^{TF}(t) D^{TF}(t); \lambda^{TF} > 0 \\
&\dot{D}^C(t) = \lambda^C r - \varsigma^C(t) D^C(t); \lambda^C < 0 \\
&\dot{\varsigma}^F(t) = \delta^F\left[D^F(t)^2 - V^F\right]; \delta^F > 0 \\
&\dot{\varsigma}^{TF}(t) = \delta^{TF}\left[D^{TF}(t)^2 - V^{TF}\right]; \delta^{TF} > 0 \\
&\dot{\varsigma}^C(t) = \delta^C\left[D^C(t)^2 - V^C\right]; \delta^C > 0 \\
&\dot{M}(t) = M(t)[g - r]
\end{aligned}
\tag{19}
$$

where r is defined as $r \equiv \lambda^M[\alpha D^F(t) + (1-\alpha)[\beta D^{TF}(t) + (1-\beta) D^C(t)]]; \alpha \in [0,1]; \lambda^M > 0$. *Equations (1)* and *(3)* imply that r is the rate of return on the asset. *System 19* has equilibrium points only for a zero-Lebesgue measure parameter set. Indeed, if the system is on an equilibrium point, $\dot{\varsigma}^F(t) = \dot{\varsigma}^{TF}(t) = \dot{\varsigma}^C(t) = 0$ and the equilibrium demands are:

$$
D^F = \pm\sqrt{V^F}\ ; D^{TF} = \pm\sqrt{V^{TF}}\ ; D^C = \pm\sqrt{V^C} \tag{20}
$$

Moreover, the rate of return is equal to the growth rate of the fundamental, so that, plugging the equilibrium demands into the equation for r, we obtain that the following equality relation between parameters must hold for the system to have equilibrium points:

$$
g = \lambda^M\left(\pm\alpha\sqrt{V^F} + (1-\alpha)\left(\pm\beta\sqrt{V^{TF}} \pm (1-\beta)\sqrt{V^C}\right)\right) \tag{21}
$$

1.2. Statistical properties

In this section, we analyze the statistical properties of the simulated time series, which have been generated by integrating the system up to time 7529 and recording the price at integer times starting

from $t = 4000$ in order to allow the system to get sufficiently close to the asymptotic dynamics and to have time series as long as the daily time series of the S&P500 index between 1 January 1990 and 31 December 2003. The system has been integrated by utilizing the default method of Mathematica 5, which switches between BFG and Adams algorithms depending on the stiffness of the system. No stochastic elements are added, because we are interested in analyzing how the interaction among different investors, whose risk aversions are time varying, may reproduce the stylized fact observed in real financial markets: volatility clustering, fat tails, no autocorrelation between returns and long memory. Thus the features of system-generated time series are endogenous and originate from the nonlinear structure of the system. The model displays statistical properties similar to those of the S&P500 index using various parameter values. In *Table 1* there are reported the mean, maximum, minimum, variance, skewness, kurtosis and the results of the Jarque-Bera test of the daily returns on the S&P500 and on the time series generated by the differential equation system with parameters and initial values reported respectively on *Table 2* and *Table 3* and identified as *Example 1* and *Example 2*. We have also reported in *Table 1* the value of the largest Lyapunov exponent for *Example 1*.[1] The distribution functions, autocorrelations of returns and square returns up to lag fifty are illustrated in *Figure 1* and *Figure 2*.

	Mean	**Maximum**	**Minimum**	**Variance**	**Skewness**	**Kurtosis**	**Jarque-Bera**	**Lyapunov exponent**
S&P 500	0.000375309	0.0573148	-0.0686674	0.000110923	-0.0163294	6.49388	1794.62	
Example 1	0.000369353	0.0587311	-0.0709184	0.000105104	0.0690029	6.59998	1908.44	0.241898
Example 2	0.000366283	0.0563845	-0.0550595	0.0000852793	0.0880204	6.2641	1325.25	

Table 1: Statistics for S&P500, *Example 1* and *Example 2* and Lyapunov exponent of *Example 1*.

	λ^M	λ^F	λ^{TF}	λ^C	α	δ^F	δ^{TF}	δ^C	V^F	V^{TF}	V^C	g	z
Example 1	60	95/15	0.25	-0.22	0.4	240000	240000	240000	1/54000	1/54000	1/54000	0.000319	0
Example 2	55	5	0.24	-0.25	0.4	240000	216000	216000	1/90000	1/90000	1/90000	0.000319	4

Table 2: Parameter values of *Example 1* and *Example 2*.

	P	F	D^F	D^{TF}	D^C	ς^F	ς^{TF}	ς^C	β
Example 1	1.1	1	$\lambda^F * \log[G(0)/P(0)]$	0	0	1	1	1	0.5
Example 2	1.1	1	$\lambda^F * \log[G(0)/P(0)]$	0	0	1	1	1	0.5

Table 3: Initial values of *Example 1* and *Example 2*.

The growth rate of the fundamental, g, is equal to the mean growth rate of S&P500, which in turn has been calculated as the rate that in a continuously compounded capitalization regime implies the same return on the index on the overall period. Since the price moves around the fundamental, the means of the simulated time series match that of the S&P500. The other parameter values have been chosen so as to give rise to statistics similar to those of the S&P500 index. In TDG, the variable that accounts for the variance is V^F, in this model variance control is much more complicated, as there exist three different types of investment strategies, each characterized by a potentially different value of V.

[1] The Lyapunov exponent of *Example* 2 is not been reported because the trajectories of the price and fundamental are unbounded and the system cannot be made stationary by performing a change of variables, therefore the Lyapunov exponent would be meaningless.

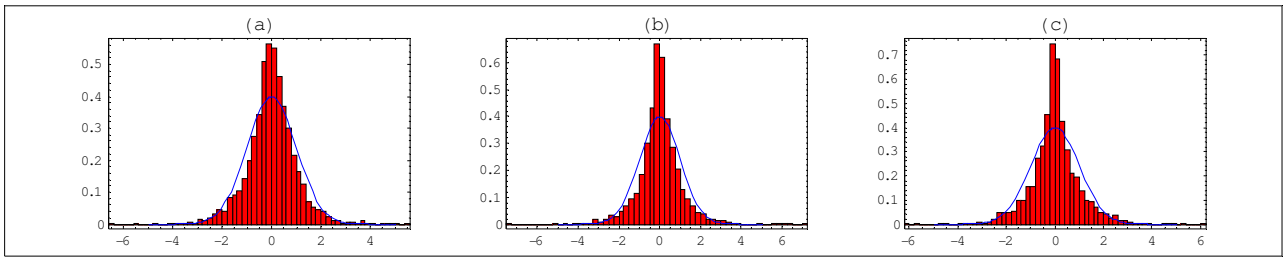

Figure 1: Standardized distributions of returns (red histograms) and standard normal distribution (blue lines) for S&P500 index from 1 January 1990 to 31 December 2003 (*a*) , Example 1 (*b*) and Example 2 (*c*).

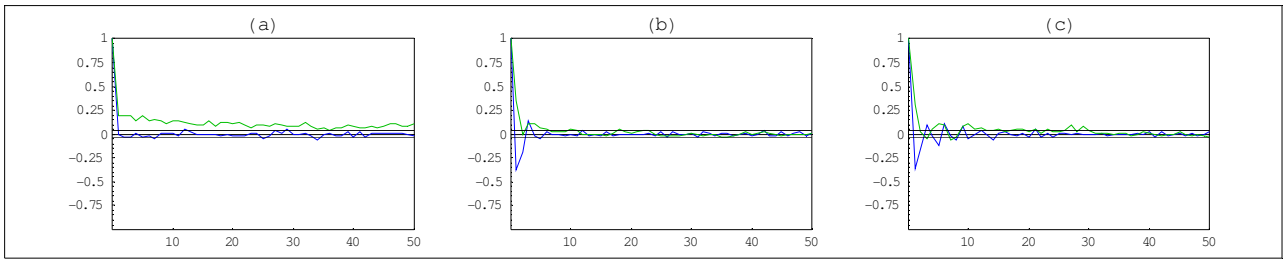

Figure 2: Autocorrelations of returns (blue lines) and square returns (green lines) for S&P500 index from 1 January 1990 to 31 December 2003 (*a*) , Example 1 (*b*) and Example 2 (*c*).

We have considered the case where trend followers and contrarians have the same values of V and δ, whereas fundamentalists may be characterized by different values, due to the smaller difference between two technical strategies than between technical and fundamentalist strategies. V^F, V^{TF}, V^C are constants because otherwise the unconditional variance would be in turn variable. For instance, the TDG setting with our specifications for the demand functions, $V = \varepsilon F$, would give rise to time series whose variance increases over time. Such a behavior is not typical of real time series, whose variances tend to be constant, unless there occur structural changes, or anyway do not follow well defined trends. V^F, V^{TF}, V^C affect not only the variance, but skewness and kurtosis as well, and the relation is not monotonic. They may even bring about a global bifurcation of the system. As pointed out by TDG, kurtosis and volatility clustering are due to the delayed reaction of investors that determines price overshooting. In a multi-agent modeling, such a process is fostered by the interaction among investors who are heterogeneous not only as concerns the time that they need to process information from the market, but also the strategies that they use to predict future prices. Real time series show little or no autocorrelation in returns and significant autocorrelations in square or absolute returns, which decay according to power laws, because of volatility clustering. Time series are also characterized by long memory and nonlinear structure. The model by TDG displays negative first order autocorrelations, close to 0.5, because of the presence of only fundamentalists that tends to drive the price back to its long period fundamental value. The introduction of trend followers should cause this autocorrelation to fall because price overshooting is more likely to occur. The action of contrarians should have less predictable effects on the autocorrelation, as these investors may offset both fundamentalists and trend followers. However the simulations give rise to significant autocorrelation that nevertheless decays very quickly. The significance of autocorrelations is due to the absence of medium and long term trends. The autocorrelations of square returns instead decay much faster than those of S&P500, because of the fact that the price moves around the exponential fundamental trend in the long run. Changes in the speed of switching between technical strategies may affect qualitatively the system dynamics, and, even in the case where the dynamics remain qualitatively unchanged, they may determine large variations in the statistical properties, even if the proportion between trend followers and contrarians remains close to 0.5. In the simulations that we have run, the smaller variance in *Example 2* is mostly due to the introduction of switching between technical strategies rather than to the decrease in V^F, V^{TF}, V^C. Kurtosis tends to rise as λ^{TF} and λ^C rise, whereas variance and skewness do not show a clear dependence on such parameters. Skewness tends to be slightly positive, conversely to the time series of the S&P500 index, which instead show a slightly negative

skewness. Positive skewness is due to the exponentially growing fundamental value that determines that large price overshooting is on average positive. Price overshooting, which also determines kurtosis in returns, is induced by both the delayed reaction of investors and the interaction between fundamentalists and trend followers, as the latter may reinforce a trend triggered by the former. On the long run, fundamentalists cause the price to growth. Contrarians' trading may not be sufficient to offset trend followers', and moreover it may happen that the demands of both trend followers and contrarians have the same sign, because of the delay in investors' reactions and the different dynamics of risk attitudes. The mean returns on time scales of 1,5,10 and 15 days are shown in *Figure 3*. It is apparent that returns cluster together on all the time scales, confirming an underlying long memory process. Such characteristics are typical of multifractal process. Let us consider a stochastic process $x(t)$ and define the increment between t and $t+\Delta t$ in the following way:

$$x(t,\Delta t) = x(t+\Delta t) - x(t)\ ;\ 0 \le t \le T\ . \tag{22}$$

Let us assume now that increments are stationary and the distribution of $x(0,\Delta t)$ is invariant with respect to time shifts. According to Mandelbrot, Fisher and Calvet (1997), a multifractal process is a continuous time process with stationary increments which satisfy:

$$E[|x(t,\Delta t)|^q] = c(q)(\Delta t)^{\tau(q)+1} \tag{23}$$

for each $t,\Delta t$ on which x is defined and for each $q \in [0, q_{\max})]$ such that $E[|x(t,\Delta t)|^q] < \infty$, where E is the expectation operator. The scaling function $\tau(q)$ determines the variations in expected value as time scale changes. Mandelbrot, Fisher and Calvet (1997) prove that scaling functions remain unchanged only for bounded time intervals, that is, multifractal processes must show transitions in their scaling properties or crossovers. Taking the logarithms of equation (23) we get:

$$\log E[|x(t,\Delta t)|^q] = \log[c(q)] + (\tau(q)+1)\log[\Delta t] \tag{24}$$

If $x(t) = \log P(t) - \log P(0)$ then $x(t,\Delta t)$ approximates the return on the time series $P(t)$ in the interval $[t, t+\Delta t]$. The plots of $\log E[|x(t,\Delta t)|^q]$ of the S&P500 and the simulated time series with respect to $\log[\Delta t]$ for q=1,1.5,2,2.5,3 are drawn in *Figure 4*. Since we are interested only in the scaling function $\tau(q)$ and not in the intercept, the values have been normalized by subtracting $\log E[|x(t,\log[10])|^q]$. Time intervals ranges from 1 to 100 days. There is no apparent crossover up to a time scale of 100 days in the time series of S&P500, thus confirming its multifractal nature. In the simulations, crossover occurs for values of t between e^3 and e^4 and the fluctuations are more erratic than those of S&P500. Such a behavior underlines the capability of the model to generate dynamics typical of a multifractal process, however the exponential growth in the fundamental value implies an exponential long run growth in the expected returns, which in turn implies that crossover occurs for smaller time intervals than those of real time series.

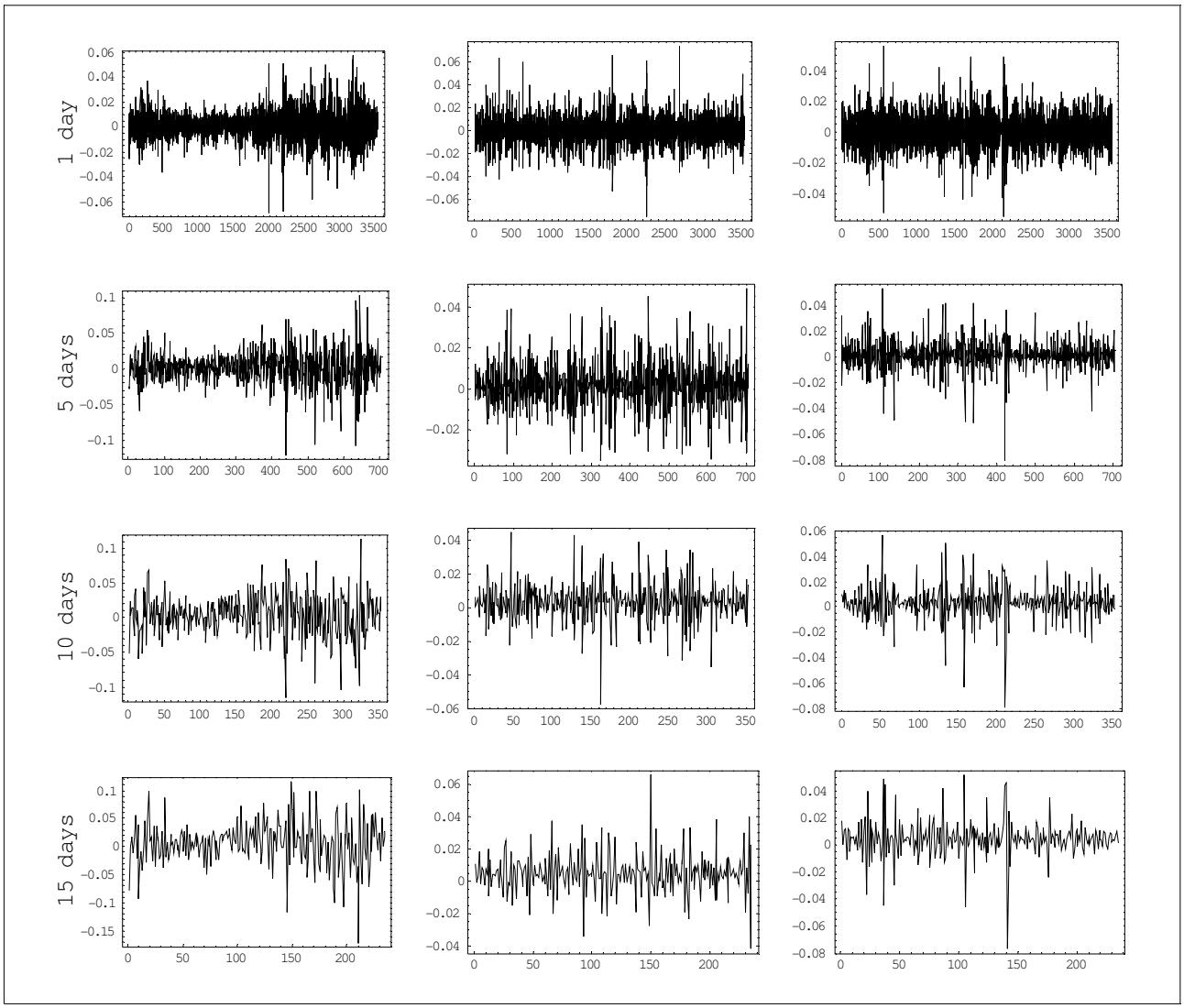

Figure 3: Time series of returns on time scales of 1, 5, 10 and 15 days on S&P500 index (left), Example 1 (middle), Example 2 (right).

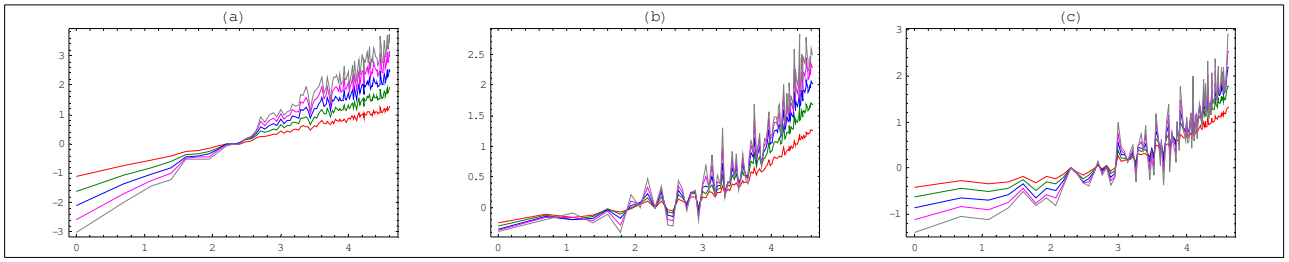

Figure 4: Plots of $\log E[|x(t,\Delta t)|^q]$ against $\log[\Delta t]$ on S&P500 index (a), Example 1 (b), Example 2 (c) for q=1,1.5,2,2.5,3 respectively in red, green, blue, purple and grey.

1.3. Comparative dynamics

In this section we will first analyze the dynamics for the system identified as *Example 1*, the dynamics for the other example being very similar, and then we will study the variations in dynamics as parameters change. In *Figure 5* there are depicted the time series in the interval $[7029,7529]$ of prices, returns, proportion of trend followers out of the total of technical traders (it is constant because z=0), demands, risk attitudes and the projection of the phase space on the planes $[D^F,\varsigma^F]$, $[D^{TF},\varsigma^{TF}]$, $[D^C,\varsigma^C]$, $[D^F,D^{TF}]$, $[D^F,D^{TF}]$, $[D^{TF},D^C]$. *Tables 4-10* show the mean, maximum, minimum, variance, skewness, kurtosis, Jarque-Bera and Lyapunov exponent for

different parameters values. From the graph of the price, two type of trends are apparent: there is an upward long period trend that matches the dynamics of the fundamental value and is due to the trading of fundamentalists and upward and downward short period trends that oscillate around the long run trend and are instead due to the trading of technical analysts as well as to the delayed reaction of the fundamentalists. Short period cycles are characterized by considerable variations in both frequency and amplitude. Such a variability is due to the heterogeneity in strategies and time horizons and is reinforced by the variability in risk attitudes. The demands of technical traders switch between positive and negative phases, differently from the fundamentalist demand, which instead tends to move around zero. The average demand of fundamentalists is slightly positive, because of the upward trend in the fundamental value. The presence of long phases of positive and negative demands of technical traders, together with the dynamics for the risk aversion may determine very large price oscillations in both directions. In fact, long phases of positive demand provoke considerable increases in price, associated with strong sales from the fundamentalists. The increase in the fundamental value triggers a stock price increase due to the purchases by fundamentalists, which is reinforced by the action of trend followers, whereas contrarians tend to sell the stock. The opposite behavior of trend followers and contrarians is shown on the projection of the phase space on the space of technical analysts' demands: the attractor is stretched along the bisector between the first and third orthant. The demand of fundamentalists has smaller oscillations in the periods where the risk aversion is high, because a high risk aversion induces the fundamentalists not to open large positions if the stock is mispriced. Whereas the risk aversion of fundamentalists follows well defined trends and is on average positive, those of technical traders tends to oscillate around zero. As such, technical traders switch between phases in which they are risk averse and phases in which are risk seekers. The dynamics for the risk attitudes may be explained in the following way: let us assume that the price is rising and the demand of trend followers is positive and greater than $\sqrt{V^{TF}}$. *Equation 15* implies that their risk aversion rises as well. The increase in price reduces the demand of fundamentalists and contrarians, but reinforces that of trend followers, which on the other hand tends to fall because of the increase in their risk aversion. Once the price falls, the demand of trend followers approaches zero (eventually becoming negative) and, as a consequence, their risk aversion falls. The dynamics are also the same in the case where the cycle is triggered by fundamentalists or contrarians. The only difference is that the demand of these investors will eventually change sign independently of their risk attitudes whereas the demand of trend followers are self-fulfilling because the price movements they induce in turn reinforce the demands, given the risk aversion. The projections of the attractor on the planes $[D^F, \varsigma^F]$, $[D^{TF}, \varsigma^{TF}]$, $[D^C, \varsigma^C]$ show the interactions between demands and risk attitudes. The different shape of the projection on the plane $[D^F, \varsigma^F]$ is due to greater amplitude and lower frequency of the dynamics of fundamentalists' risk aversion than those of the other investors. In any case, however, risk attitudes may vary considerably even during phases in which the demands are almost steady. Indeed it is sufficient that the absolute value of the demand of investors type *i* remains for a long time respectively above $\sqrt{V^i}$ to get a considerable change in risk aversion. The time derivatives of the risk attitudes tend to reach their lower bounds, which are respectively equal to $-\delta^F V^F$, $-\delta^{TF} V^{TF}$ and $-\delta^C V^C$, only when the demands are very close to zero.

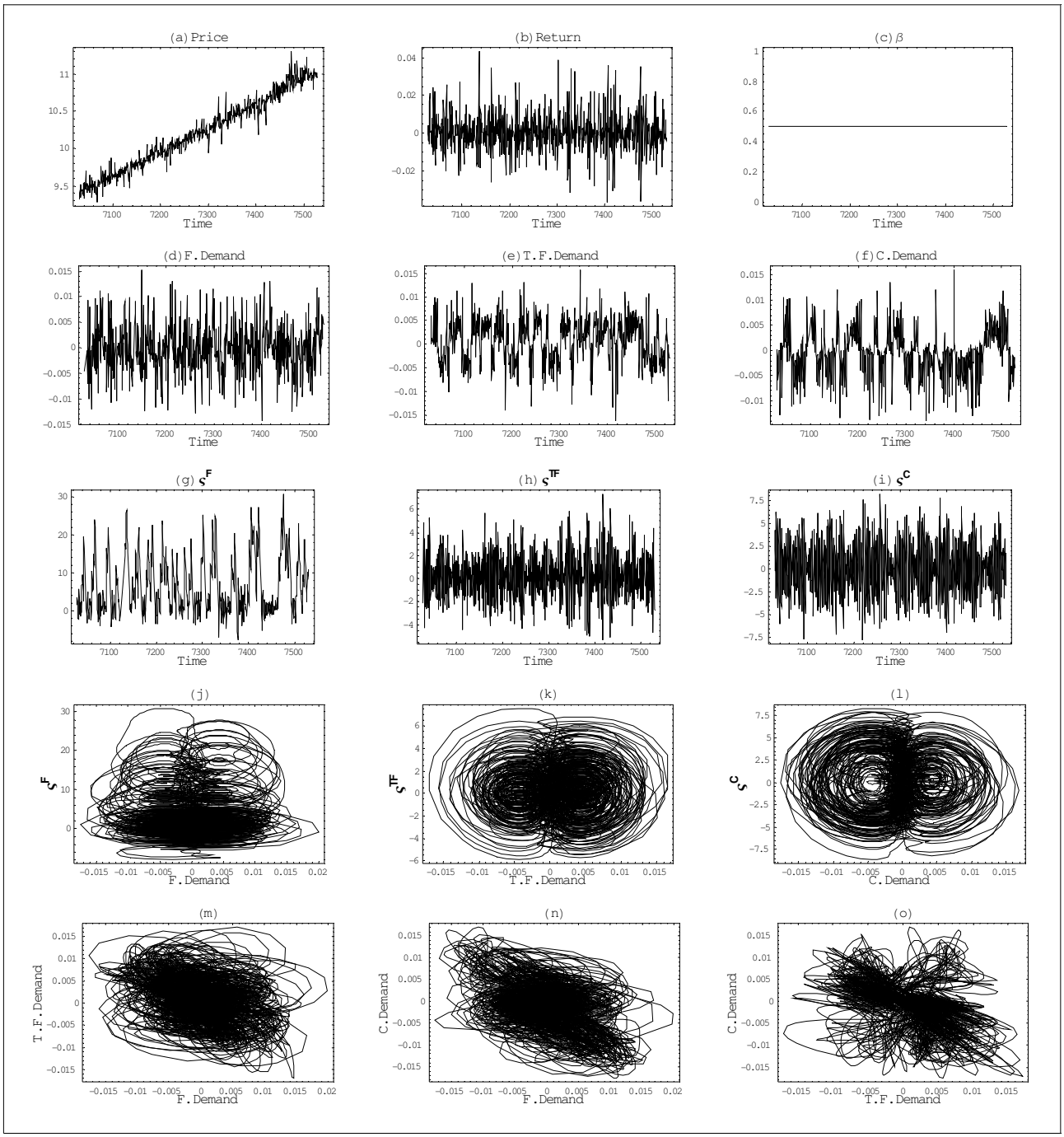

Figure 5: Time series of prices (*a*), returns (*b*), proportion of trend followers of technical traders (*c*), demand of fundamentalists (*d*), trend followers (*e*), contrarians (*f*), risk aversion of fundamentalists (*g*), trend followers (*h*), contrarians (*i*), projections of the phase space on the planes $[D^F, \varsigma^F]$ (*j*), $[D^{TF}, \varsigma^{TF}]$ (*k*), $[D^C, \varsigma^C]$ (*l*), $[D^F, D^{TF}]$ (*m*), $[D^F, D^{TF}]$ (*n*), $[D^{TF}, D^C]$ (*o*) for the time interval [7029,7529].

1.3.1 Effects of changing the proportion of fundamentalists and technical traders. In order to analyze the effect of the proportion of fundamentalists and technical traders, we select values of α ranging from 0 to 1 and with a difference of 0.1 between a simulation and the next. If there are no fundamentalists or if their proportion is only ten percent, the price goes to infinity, because technical trading drives the price away from the fundamental.[1] If $\alpha = 0.2$ the fundamentalists are able to steer the price to the fundamental value, but prices are subject to large oscillations induced by technical traders. Such oscillations become larger and larger as time goes on. In fact larger departures from the fundamental value are needed for the fundamentalists to bring the price back

[1] The price goes to zero with other parameter values. What matters here is that the price does not match the fundamental in the long run.

close to the fundamental value. The dynamics for the fundamentalist demand differ considerably from the baseline case where $\alpha = 0.4$, in fact the departure from the fundamental value brings about long phases in which the fundamentalists go either long or short on the asset, determining in this way an increase in their risk aversion. This in turn implies a lower capability of offsetting technical traders. The overall demand of the latter presents long phases in which the demand is either positive or negative, phases in which it changes sign quickly and phases where the demands of contrarians and trend followers offset each other. This latter feature is called synchronization in the dynamical systems literature. During phases of synchronization the system reduces by one dimension. When the technical demand is equal or close to zero, fundamentalists bring the price back close to the fundamental value. As a consequence of the fact that the total demand does not change sign for long periods, the price tends to follow a monotonic trajectory when it is far from the fundamental and to oscillate as it gets close to it. Thus, the synchronization of technical traders determines an intermittent behavior in the system with regular monotonic phases interrupted by chaotic bursts. The time series of fundamentalist and technical demands are depicted in *Figure 6*. If α is equal to 0.3 the proportion of fundamentalist is sufficiently high as to prevent technical trading from bringing about larger and larger departures from the fundamental value. The oscillations have anyway larger amplitudes than in the case where $\alpha = 0.4$, and this in turn determines an increase in the variance and a decrease in the kurtosis. If fundamentalists account for half of the investors, the demand of technical traders is generally lower than in the baseline case because fundamental trading prevents strong changes in the price. This leaves little room for a persistent phase of fundamentalist demand and therefore fundamentalists are more likely to became risk seekers. The higher proportion of fundamentalists determines a more regular behavior of the system, as denoted by the decrease in kurtosis. If the fraction of fundamentalists is equal to or greater than sixty percent, the system no longer converges to a strange attractor. Furthermore, the only attracting invariant set is a quasi-periodic attractor, as denoted by the values of the Lyapunov exponents. Moreover, as the proportion of fundamentalists in the market increases, the amplitude of the oscillations reduces. If there are only fundamentalists the attractor becomes strange again and the Lyapunov exponent rises up to 0.523002, which would indicate a highly chaotic system. However the rise in the Lyapunov exponent is due to the increase in the amplitudes of the oscillations that in turn are due to the overreaction induced by the delayed reaction of fundamentalists, which brings price above (below) the fundamental price when the security is originally underpriced (overpriced).

1.3.2. Effects of changing the growth rate of the fundamental value. Increases in *g* cause a stronger activity of the fundamentalists on the market. The price tends to remain close to the fundamental value and the amplitude of the price oscillations is smaller, therefore the variance decreases as *g* increases. If *g* is four times greater than in the baseline case the action of fundamentalists is so strong as to break the strange attractor into a limit cycle. If *g* is five times greater, the system converges to a quasi-periodic attractor. The attractor is a limit cycle for *g* equal to or greater than six times the baseline case.

α	Mean	Maximum	Minimum	Variance	Skewness	Kurtosis	Jarque-Bera	Lyapunov exponent
0.2	0.00210084	0.281998	-0.223493	0.00347306	0.657885	4.55161	608.396	
0.3	0.000902394	0.161515	-0.115126	0.00117017	0.151231	3.91785	137.289	0.268056
0.4	0.000369353	0.0587311	-0.0709184	0.000105104	0.0690029	6.59998	1907.9	0.241898
0.5	0.00034002	0.0309093	-0.0298682	0.0000438907	0.164723	5.05137	634.548	0.175174
0.6	0.000505747	0.0351398	-0.032607	0.000360944	0.0181459	1.57432	298.98	0.0989546
0.7	0.000542628	0.0235851	-0.0309212	0.000432451	0.0149926	1.50448	328.907	0.0288602
0.8	0.000425532	0.0235851	-0.0225013	0.000227566	0.0137007	1.50864	327.061	0.0345303
0.9	0.000323392	0.00685721	-0.00633042	0.0000171097	0.0046185	1.51802	322.865	0.0124616
1	0.000502513	0.108746	-0.0974863	0.000367779	0.397363	15.0274	21357.8	0.523002

Table 4: Mean, maximum, minimum, variance, skewness, kurtosis, Jarque-Bera and Lyapunov exponent for *Example 1* as α varies from 0.2 to 1. The Lyapunov exponent is not reported for α=0.2 because is meaningless when the dynamics are not bounded.

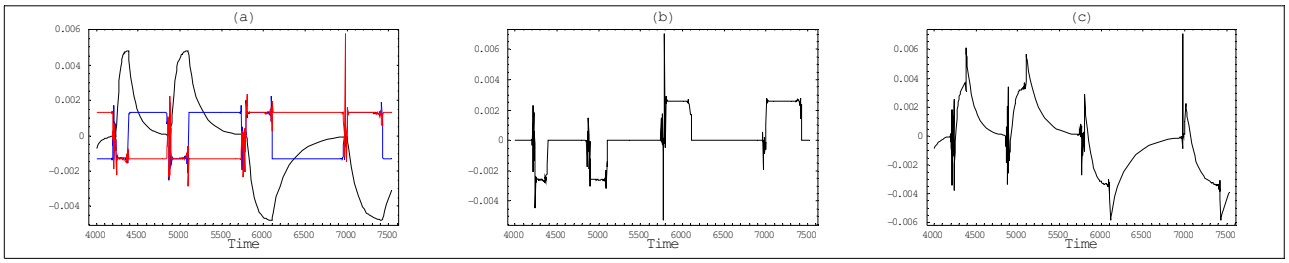

Figure 6: In *Panel a* there are represented the total demands of fundamentalist (in black), trend followers (in blue) and contrarians (in red) respectively given by αD^F, $(1-\alpha)\beta D^{TF}$ and $(1-\alpha)(1-\beta)D^C$ when $\alpha = 0.2$ and $\beta = 0.5$. In *Panel b* there is depicted the total technical demand, given by the sum of the demands of trend followers and contrarians. Total excess demand, given by equation (3), is depicted in *Panel c*. Time interval ranges from 4000 to 7529.

$\frac{g}{0.000319}$	Mean	Maximum	Minimum	Variance	Skewness	Kurtosis	Jarque-Bera	Lyapunov exponent
0	0.0000537886	0.0495222	0.0452839	0.000118037	0.027382	5.16913	692.095	0.252298
1	0.000369353	0.0587311	-0.0709184	0.000105104	0.0690029	6.59998	1907.9	0.241898
2	0.000684626	0.0610451	-0.0564503	0.0000919609	0.109867	5.82433	1179.69	0.224348
3	0.000994219	0.0414887	-0.0391781	0.0000699423	0.124856	5.70547	1085.14	0.204809
4	0.00129316	0.0191797	-0.0148457	0.0000362081	0.342639	3.63877	129.012	0.00105954
5	0.00159735	0.00478863	-0.00147119	$(2.93407)10^{-6}$	0.0557558	1.81467	208.364	0.00214585
6	0.00191871	0.00426463	-0.000423662	$(2.72064)10^{-6}$	-0.00054509	1.50511	328.501	0.00123471

Table 5: Maximum, minimum, variance, skewness, kurtosis, Jarque-Bera and Lyapunov exponent for *Example 1* as g varies from 0 to 6·0.000319.

1.3.3. Effects of changing the speed of adjustment of the market maker. A higher value of the speed of reaction of the market maker determines a greater response of the price to a given excess demand and this in turn brings about an increase in the variance. This in turn determines a greater disorder in the system. For instance, if $\lambda^M = 20;40$ the trajectories are periodic, if $\lambda^M = 10;30$ the attractor is strange but more tidy than in the standard case. Indeed, the Lyapunov exponents are respectively equal to 0.0021286 and 0.0012897 and the return distributions are approximately normal. In *Figures 7* and *8* there are reported the phase plots respectively for λ^M equal to 20 and 30.

1.3.4. Effects of changing the speed of expected price adjustment of fundamentalists. Increasing the speed reaction of fundamentalists brings about a decrease in the variance because the price tends to stay close to the fundamental. The system undergoes a transition as the parameter λ^F is increased, that is, the dynamics shows a cyclical behavior after a transient chaotic phase. This kind of transition, called attractor destruction, is a type of crisis-induced intermittency and has been investigated by Grebogi, Ott, Romeiras and Yorke (1986) and Grebogi, Ott, Romeiras and Yorke (1987). However, for large values of λ^F the attractor becomes strange again; if $\lambda^F = 40$ the Lyapunov exponent is 0.127318, that is, the system is weakly chaotic due to the overreaction of fundamentalists. This case is similar in some respects to that where there are only fundamentalists on the market, indeed kurtosis rises up to 10.1876. Because of the presence of technical traders, which are affected by the changes in prices triggered by the fundamentalists, it is not possible to determine what the dynamics eventually are as the reaction speed of the fundamentalists is further increased. For instance, if $\lambda^F = 190$ the dynamics are periodic, but if $\lambda^F = 300$ the attractor is strange, with a Lyapunov exponent of 0.240876, and is characterized by an intermittent behavior.

λ^M	Mean	Maximum	Minimum	Variance	Skewness	Kurtosis	Jarque-Bera	Lyapunov exponent
10	0.000330484	0.0206878	-0.0201229	0.0000253034	0.0387064	3.48532	35.505	0.183651
20	0.000360739	0.0176783	-0.0168995	0.0000794659	0.170052	1.97156	172.483	0.0021286
30	0.000365441	0.0331703	-0.0319962	0.000081857	0.017598	3.02064	0.24473	0.159328
40	0.000357116	0.014606	-0.0172128	0.0000779788	-0.206538	1.9594	184.261	0.0012897
50	0.000361973	0.0197733	-0.0142528	0.0000844143	0.241145	2.0067	179.23	0.0014726
60	0.000369353	0.0587311	-0.0709184	0.000105104	0.0690029	6.59998	1907.9	0.241898
70	0.000381041	0.0793545	-0.0628766	0.000128775	0.145983	7.13087	2520.95	0.233348
80	0.000405412	0.0669915	-0.0570457	0.000172349	0.157421	4.88388	536.273	0.235278
90	0.00041944	0.0631928	-0.0533371	0.000204906	0.0882721	4.03829	163.054	0.257029
100	0.000425154	0.0978468	-0.0698592	0.000234512	0.160142	4.68113	430.533	0.250071

Table 6: Maximum, Minimum, Variance, Skewness, Kurtosis, Jarque-Bera and Lyapunov exponent for *Example 1* as λ^M varies from 10 to 100.

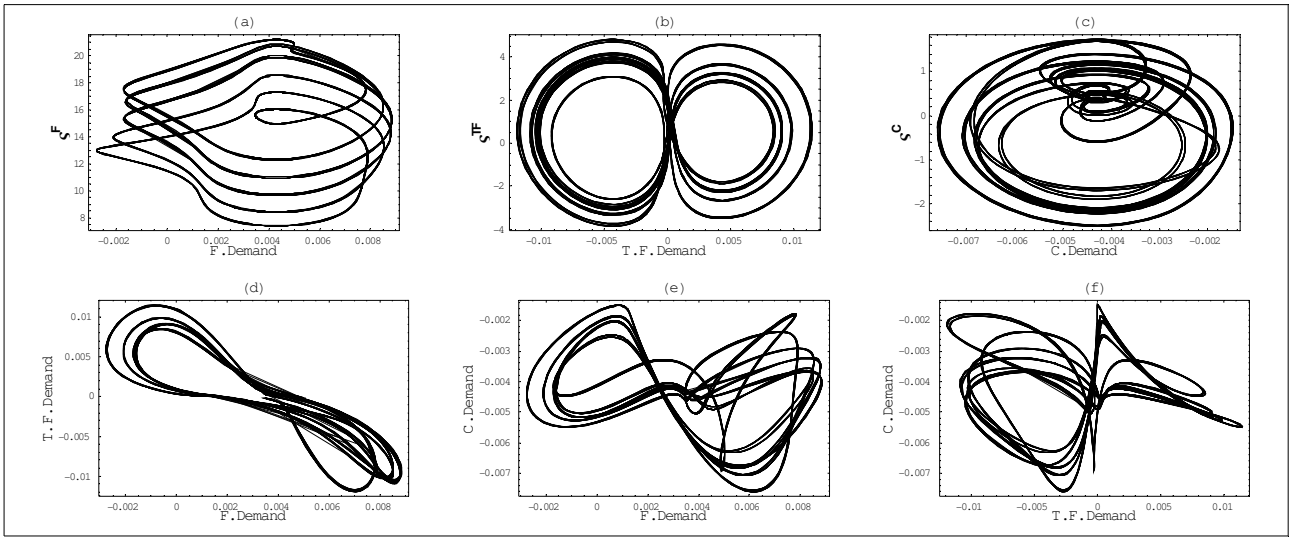

Figure 7: Projections of the phase space on the planes $[D^F, \varsigma^F]$ (*a*), $[D^{TF}, \varsigma^{TF}]$ (*b*), $[D^C, \varsigma^C]$ (*c*), $[D^F, D^{TF}]$ (*d*), $[D^F, D^{TF}]$ (*e*), $[D^{TF}, D^C]$ (*f*) when $\lambda^M = 20$.

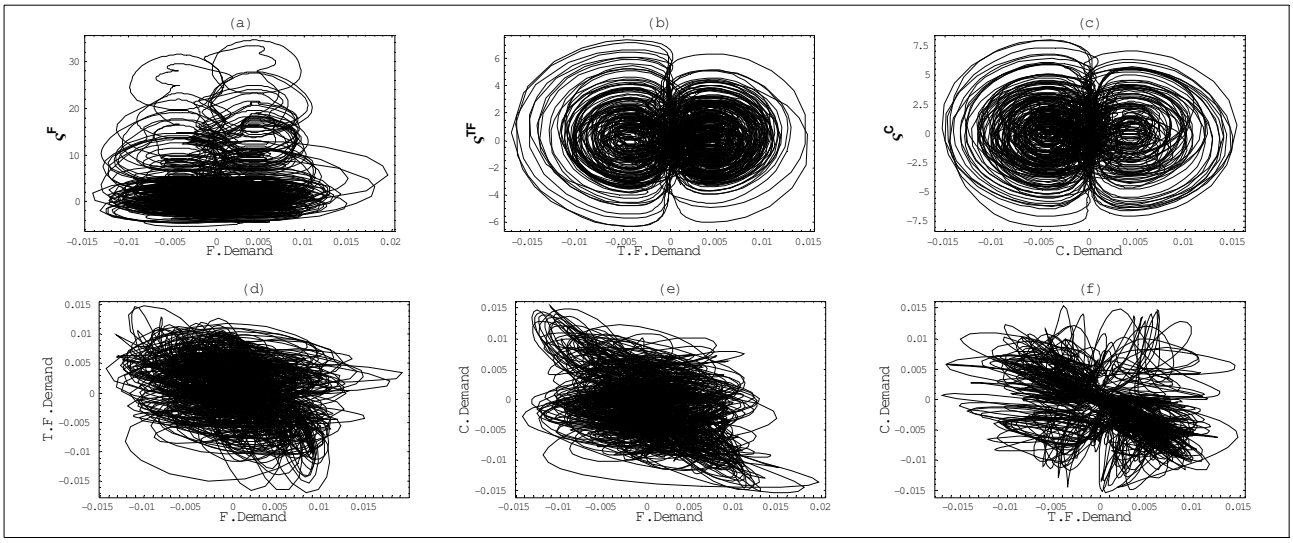

Figure 8: Projections of the phase space on the planes $[D^F, \varsigma^F]$ (*a*), $[D^{TF}, \varsigma^{TF}]$ (*b*), $[D^C, \varsigma^C]$ (*c*), $[D^F, D^{TF}]$ (*d*), $[D^F, D^{TF}]$ (*e*), $[D^{TF}, D^C]$ (*f*) when $\lambda^M = 30$.

λ^F	Mean	Maximum	Minimum	Variance	Skewness	Kurtosis	Jarque-Bera	Lyapunov exponent
19/15	0.00055803	0.0825522	-0.0761281	0.000483397	0.101521	3.75793	90.5049	0.260045
38/15	0.00048943	0.0905994	-0.0713038	0.000324588	0.0888249	3.6847	73.5548	0.20373
57/15	0.000434872	0.054647	-0.054509	0.000234301	0.0296036	3.25936	10.4036	0.243968
76/15	0.000398758	0.0697828	-0.0714307	0.000157999	0.174213	5.02767	622.226	0.247527
95/15	0.000369353	0.0587311	-0.0709184	0.000105104	0.0690029	6.59998	1907.9	0.241898
114/15	0.000370917	0.0694991	-0.0494394	0.000104576	0.236946	6.56116	1897.24	0.232318
133/15	0.000368247	0.0610275	-0.0395701	0.0000912715	0.256507	3.44351	67.603	0.00113966
152/15	0.000368016	0.0736272	-0.0701349	0.0000930663	0.213145	4.98602	606.522	0.00244454
171/15	0.000356914	0.0190932	-0.0147682	0.0000847965	0.163268	1.78405	233.018	0.00236142
190/15	0.000352543	0.0593143	-0.0400121	0.0000674469	0.145138	6.65448	1975.6	0.064413
40	0.000327483	0.0215197	-0.0206138	0.0000167665	0.0946897	10.1879	7602.37	0.127318
190	0.000373124	0.0427878	-0.0428233	0.000112505	0.158359	4.63448	407.577	0.0739194
300	0.000472087	0.0845286	-0.0675717	0.000316402	0.273594	4.19152	252.783	0.240876

Table 7: Maximum, Minimum, Variance, Skewness, Kurtosis, Jarque-Bera and Lyapunov exponent for *Example 1* as λ^F varies from 19/15 to 190/15 and for λ^F equal to 30, 190, 300.

1.3.5. Effects of changing the extrapolation speed of trend followers and contrarians. From the values of the Lyapunov exponent, it is apparent that for low values of λ^{TF} and λ^C the system

converges to a limit cycle. The dynamics may explode or converge to a price equal to zero if contrarians are much more reactive than trend followers, as in the cases where $\lambda^{TF} = 0.16; 0.17; 0.19$. This result is due to the risk aversion dynamics that cause the demands of trend followers and contrarians to have the same sign, because contrarians become risk seekers or not sufficiently risk averse to offset the trend followers. The price diverges to infinity or converges to zero when the demand of technical traders remains positive or negative (in these cases the statistics are meaningless and therefore are not reported in *Table 8* and *9*). When the system converges to a strange attractor, the statistics do not show a clear dependence on λ^{TF} and λ^{C}. Skewness tends to be slightly positive, differently from the time series of the S&P 500 index, which is instead slightly negative skewed. Positive skewness is due to the short term overshooting, as explained in *Section 3*. Overshooting, which causes also kurtosis in the time series, is induced by both the delayed reaction of investors and the interactions between fundamentalists and trend followers, since the latter may reinforce a trend triggered by the action of the former and contrarian trading is not sufficient to offset the trend followers. If we increase the reactivity of technical traders, the system becomes more regular, as trend followers and contrarians tend to balance each other. The dynamics are less regular if we only increase the reaction parameter of trend followers, because they prevail over contrarians.

1.3.6. Effects of switching between trend following and contrarian strategies. So far we have dealt with a model where the proportion between trend followers and contrarians are kept constant. If $z > 0$ such proportions become path dependent. The higher the value of *z*, the higher the fraction of trend followers because this strategy is generally more profitable than the contrarian one, since price grows in the long run. This higher presence of trend chasers may render the system chaotic.

λ^{TF}	Mean	Maximum	Minimum	Variance	Skewness	Kurtosis	Jarque-Bera	Lyapunov exponent
0.15	0.000384673	0.0187929	-0.0242905	0.000135443	-0.355236	2.13223	184.895	0.00263052
0.16	-	-	-	-	-	-	-	-
0.17	-	-	-	-	-	-	-	-
0.18	0.000372227	0.0173602	-0.0222974	0.000117359	-0.290264	2.03177	187.349	0.0010877
0.19	-	-	-	-	-	-	-	-
0.20	0.000378055	0.0598837	-0.0553325	0.000117933	0.133162	6.00388	1336.85	0.201067
0.21	0.00038489	0.122849	-0.0810554	0.000131612	0.387327	10.6243	8633.27	0.221105
0.22	0.000369102	0.0272894	-0.0259532	0.0000990937	0.037827	3.71217	75.3983	0.209684
0.23	0.000367604	0.0593017	-0.0495785	0.0000994084	0.146344	6.06788	1396.14	0.238593
0.24	0.000366941	0.0481003	-0.0573432	0.0000990906	-0.00316219	5.81994	1168.96	0.237215
0.25	0.000369353	0.0587311	-0.0709184	0.000105104	0.0690029	6.59998	1907.9	0.241898

Table 8: Maximum, Minimum, Variance, Skewness, Kurtosis, Jarque-Bera and Lyapunov exponent for *Example 1* as λ^{TF} varies from 0.15 to 0.25.

λ^{C}	Mean	Maximum	Minimum	Variance	Skewness	Kurtosis	Jarque-Bera	Lyapunov exponent
-0.15	0.000369556	0.0213667	-0.0158433	0.000106152	0.179352	1.91581	191.707	0.0021656
-0.16	0.000372044	0.0211957	-0.015605	0.000102849	0.181869	1.92979	187.815	0.0024273
-0.17	0.000370366	0.0210591	-0.0156312	0.000099644	0.186281	1.95433	181.137	0.0026694
-0.18	0.000380905	0.0478136	-0.0481585	0.000121981	0.0891421	4.88654	527.85	0.230824
-0.19	0.000377074	0.0465356	-0.0424717	0.000115556	0.0318894	4.71706	433.996	0.226468
-0.20	0.000376226	0.0505584	-0.0478036	0.000109272	0.105942	5.21538	728.061	0.246516
-0.21	0.00036901	0.0523215	-0.0468544	0.0000991786	0.11308	5.38548	844.025	0.233281
-0.22	0.000369353	0.0587311	-0.0709184	0.000105104	0.0690029	6.59998	1907.9	0.241898
-0.23	0.000369951	0.0864171	-0.0585479	0.000102825	0.138732	6.8382	2176.89	0.213399
-0.24	0. 0.000376719	0.0723912	-0.0645418	0.000114519	0.047148	7.25154	2658.42	0.227939
-0.25	0.000396688	0.0706271	-0.0654394	0.000159497	0.263336	15.3175	22343.7	0.158465

Table 9: Maximum, Minimum, Variance, Skewness, Kurtosis, Jarque-Bera and Lyapunov exponent for *Example 1* as λ^{C} varies from -0.15 to -0.25.

Let us consider the case with constant proportion where $\lambda^{TF} = 0.16$ and $\lambda^{C} = -0.15$. The system converges towards a limit cycle. If $z = 50$ the system, after an initial chaotic phase, until $t \approx 1000$, approximates a regular orbit very similar to the limit cycle obtained with constant proportion and

eventually becomes chaotic as $t \approx 6600$. Indeed, the dynamics approximate a limit cycle as long as the proportion remains close to 0.5. The phase space projections of the system in the time interval $[2000,2200]$ are represented in *Figure 9*. The fraction of trend followers is on average equal to 0.503711 and tends to oscillate between 0.48 and 0.54 with a variance of 0.000248758. If $z = 100$ there are larger oscillations in the composition of technical analysts. Indeed, while the mean of the fraction of trend followers remains slightly over half (0.508117), the variance increases up to 0.00264788.[1] The higher proportion of trend followers causes greater departures from the fundamental value triggering a reaction by all types of investors. Such dynamics bring about an increase in the variance and the kurtosis of returns. If z is increased up to 150 and subsequently up to 500, the oscillations in the proportion between technical traders become larger and the variance of returns increases further, while kurtosis decreases because the increase in variance determines that some returns previously in the tails of the distribution now approach the center.

z	Mean	Maximum	Minimum	Variance	Skewness	Kurtosis	Jarque-Bera	Lyapunov exponent
0	0.000419108	0.0204648	-0.0259058	0.000187242	-0.184689	1.7386	253.951	0.00137831
50	0.000420392	0.0568036	-0.0711078	0.000191746	-0.16719	2.8211	21.1409	
100	0.000467982	0.0851743	-0.164496	0.000304584	-0.035824	8.06507	3772.03	
150	0.000565746	0.126586	-0.125605	0.000493903	0.122439	6.1863	1501.23	
500	0.000994454	0.154838	-0.128476	0.00136727	0.222942	4.19228	238.189	

Table 10: Maximum, Minimum, Variance, Skewness, Kurtosis, Jarque-Bera and Lyapunov exponent for *Example 1* for z equal to 0, 50, 100, 150, 500.

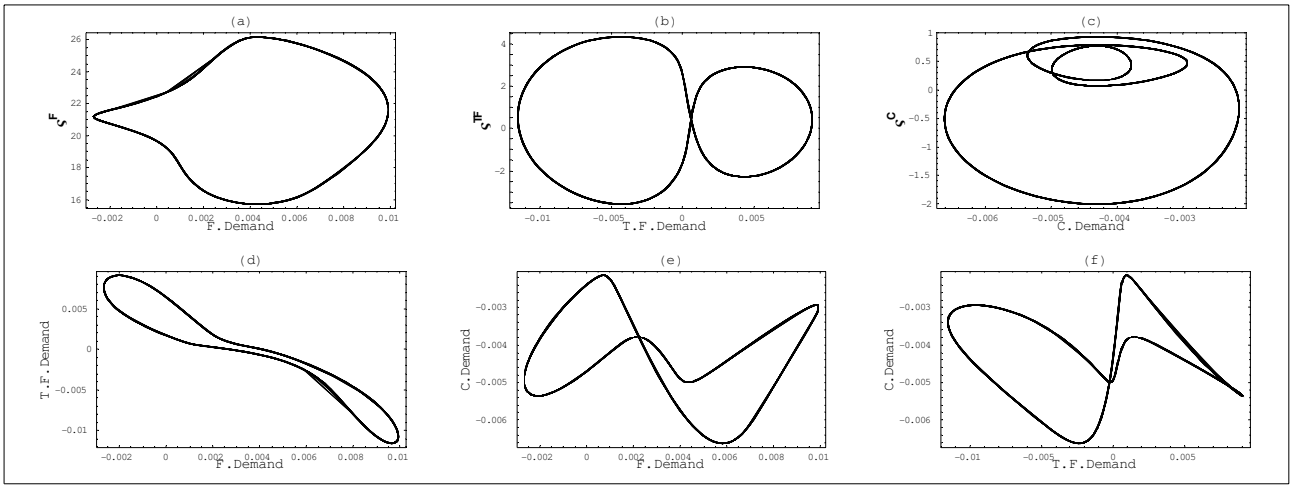

Figure 9: Projections of the phase space on the planes $[D^F, \varsigma^F]$ (*a*), $[D^{TF}, \varsigma^{TF}]$ (*b*), $[D^C, \varsigma^C]$ (*c*), $[D^F, D^{TF}]$ (*d*), $[D^F, D^{TF}]$ (*e*), $[D^{TF}, D^C]$ (*f*) when $\lambda^{TF} = 0.16$, $\lambda^C = -0.15$ and z=50 in the time interval [2000,2200].

1.3.7. Effects of introducing a feedback between real and financial sectors. We assume that the fundamental value is affected by the asset price. The economic rationale is that a higher price boosts consumption and, as a consequence, the real economy as a whole. We assume that the dynamics of the fundamental follows the differential equation:

$$\frac{\dot{F}(t)}{F(t)} = g + m\frac{P(t)}{F(t)}; m = 0.5 \tag{25}$$

The introduction of this kind of feedback induces a unit root behavior in the price time series with scaling properties very to those of S&P500. This is apparent from *Figure 10* where there are reported the simulated time series and the plot of $\log E[|x(t,\Delta t)|^q]$ against $\log[\Delta t]$. Indeed the R^2 values

[1] The mean and variance of trend followers are computed in the time interval from 4000 and 7529, as the statistics of time series of returns.

are $R^2(q=1)=0.986382,\ R^2(q=1.5)=0.987\,,R^2(q=2)=0.987352,\quad R^2(q=2.5)=0.98752,$ $r^2(q=3)=0.987641\,.$

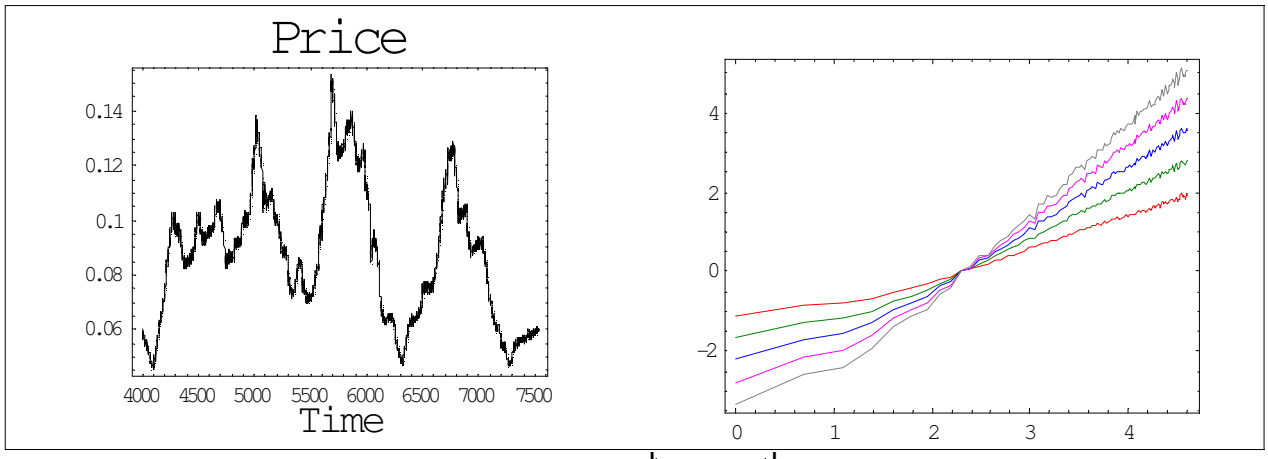

Figure 10: Time series of price (left panel) and plot of $\log E\left[\left|x(t,\Delta t)^q\right|\right]$ against $\log[\Delta t]$ with price-fundamental feedback.

2. A Model of Heterogeneous Traders with State-Dependent Switching of Strategies

2.1. The model

Let us consider a financial market where at each time unit a risky and a risk-free assets are traded. The market is composed of three different type of investors: fundamentalists, trend followers and contrarians. Let $W_{i,t}$ be the wealth of investor type *i* in period *t*, *P* and *F* be the logarithms of the price and fundamental value of the risky asset, *g* the interest rate paid by the risk-free asset and $z_{i,t-1}$ the proportion of wealth the investors type *i* invest in the risky asset. The wealth of investor *i* at time *t* is given by:

$$W_{i,t} = W_{i,t-1} + W_{i,t-1}\left(1 - z_{i,t-1}\right)g + W_{i,t-1}z_{i,t}\left(P_{i,t} - P_{t-1}\right) \tag{1}$$

Chiarella and He (2001) proved that the optimum proportion of risky asset at time *t* obtained by maximising the expected utility of wealth at time *t+1* is approximated by the following:

$$\pi_t = -\frac{E_{t,t+1}\left(P_{t+1} - P_t\right) - g}{\sigma^2_{t,t+1}\left(P_{t+1} - P\right)} \frac{U'\left(W_t\right)}{W_t U''\left(W_t\right)}.$$

where δ_i is respectively the risk aversion of investor *i* and $\sigma^2_{i,t,t+1}\left(P_{t+1} - P_{i,t}\right)$ is the expected variance of the return on the risky asset at the next period predicted by the investor. Therefore, if each traders maximize the expected value of a CARA utility function $-\exp\left[-\delta_i W_{i,t}\right]$, the solution to the optimization problem leads to the following dollar value demand for the risky asset:

$$D_{i,t} = \frac{E_{i,t,t+1}\left(P_{t+1} - P_t\right) - g}{\delta_i \sigma^2_{i,t,t+1}\left(P_{t+1} - P_{i,t}\right)}; \delta_i > 0 \tag{2}$$

as proved by Chiarella and He (2001). Alternatively, the same solution is obtained in terms of wealth proportions if we assume that the market is composed of homogeneous investors who allocate their wealth according to fundamentalist, trend following and contrarian strategies and maximize the following CRRA utility function:

$$U(W) = \begin{cases} \frac{1}{1-\delta}\left(W^{1-\delta} - 1\right); \delta \neq 1 \\ \log(W); \delta = 1 \end{cases}.$$

This assumption of CRRA utility function maximization lead to a market where at each period every agent allocate their wealth across three different strategies with proportions that are the same for each investors. Let D_f be demands of fundamentalists, trend followers and contrarians respectively. The fundamentalist prediction of the returns on the risky asset at time t estimated at time *t-1* by assuming that the returns will be proportional to the difference between the logarithms of fundamental and price:

$$E_{f,t,t-1} = \eta\left(F_{t-1} - P_{t-1}\right); \eta \in (0,1). \tag{3}$$

Thus, the fundamentalists assume that price will mean-revert in the long run to the fundamental value with a speed determined by the value of η. Indeed *Equation (3)* implies that, if investors believe that the fundamental is constant, $E_{f,t+1,t}(F_{t+1} - P_{t+1}) = (1-\eta)(F_t - P_t)$.[1] We assume that the fundamentalist risk aversion and estimated variance are constant. The estimation of variance by the trend followers and contrarians is instead an increasing function of the absolute value of the estimated excess return. This assumptions has a stabilizing effect on the system because it tends to prevent trend followers from triggering self-generated prophecies that will drive the price to infinity or zero when $|\psi_{tf,t} - g|$ becomes large. Following Chiarella, Dieci, Gardini (2002) we assume that chartist demand is specified by a function $h(\psi_{j,t} - g); j = tf, c$ such as *h'*>0, *h*(0)=0, there exist a value of the expected excess return $q^* = (\psi_{j,t} - g)^*$ such that *h''*<0 (>0) for all $(\psi_{j,t} - g) > q$ $((\psi_{j,t} - g) < q)$ and $\lim_{\psi \to \pm\infty} h'(\psi_{i,t} - g) = 0$. We assume the following functional form for *h*:

$$D_{j,t} = \gamma_j \arctan[\theta_j(\psi_{j,t,t+1} - g)]; j = tf, c \tag{4}$$

where the subscripts *tf* and *c* identify the trend followers and contrarians. $\psi_{tf,t,t+1}$ and $\psi_{c,t,t+1}$ are the expected returns of the technical traders on the risky asset, which are updated as a weighted average of current estimation and respectively return, if traders are trend followers, or the opposite of return, if traders are contrarians, that is:

$$\begin{aligned} \psi_{tf,t,t+1} &= (1-c_{tf})\psi_{tf,t-1,t} + c_{tf}(P_{i,t} - P_{i,t-1}); c_{tf} \in (0,1) \\ \psi_{c,t,t+1} &= (1-c_c)\psi_{c,t-1,t} - c_c(P_{i,t} - P_{i,t-1}); c_c \in (0,1) \end{aligned} \tag{5}$$

The market is composed of a fraction $n_{f,t}$ of fundamentalists and $n_{tf,t}$ of trend followers. This implies that the fraction of contrarians is $1 - n_{f,t} - n_{tf,t}$. Conversely to the majority of the literature on heterogeneous agent modelling, where the current holdings of the assets is not taken into account when defining the market excess demand, we assume more realistically that it is given by the difference between the optimal and actual holdings of the assets of all types of investors. Therefore the market demand is approximated by:[2]

$$\xi_t = n_{f,t}D_{f,t} + n_{tf,t}D_{tf,t} + n_{c,t}D_{c,t} - (n_{f,t-1}D_{f,t-1} + n_{tf,t-1}D_{tf,t-1} + n_{c,t-1}D_{c,t-1}) \tag{6}$$

The market is cleared by the action of a market maker who offset the imbalances in market demand by taking an offsetting short (long) position on the risky asset if market excess demand is positive (negative). The market maker adjust the price as a function of the market demand and the mispricing of the asset, pursuing in this way also a stabilizing actions. The log-price change is given by the following linear difference equation:

$$P_{t+1} - P_t = \beta\xi_t + \alpha(F_t - P_t); \beta > 0 \tag{7}$$

---

[1] This applies if the fundantamentalists believe that the fundamental is constant. This result still holds if the fundamentalists believe that fundamental is time-varying by adding the expected fundamental change to *Equation (3)*.

[2] We do not consider that the value of the previous period holdings changes because of the variation in the price of the risky asset occurring between two consecutive trading periods. Such changes tends to be negligible as the trading period become smaller.

where α and β measures the speed of reaction of the market maker with respect to market excess demand and mispricing. The fundamental grows exponentially at a rate ϕ, therefore F evolves according to the following equation:

$$F_{t+1} = F_t + \phi \tag{8}$$

We assume that the more profitable is strategy, the more investors will switch to that strategy. Following Brock and Hommes (1997,1998) and Brock, Hommes, Wagener (2001) the proportions of agents who trade according to strategy *i* evolves according to an evolutionary fitness measure $U_{i,t}$. This fitness measure is subject to an IID noise generated by a double exponential distribution. This assumptions imply that as the number of agents goes to infinity, the probability that an agent trades according to strategy *i* is given by the following "Gibbs" probability:

$$n_{i,t} = \frac{\exp\left[-\lambda U_{i,t}\right]}{\sum_j \exp\left[-\lambda U_{j,t}\right]}; \lambda > 0 \tag{9}$$

$U_{i,t}$ depends inversely on the fitness of a strategy. Agents tend to switch to the prediction rule that has the highest fitness. λ is the intensity of choice and measure the speed of switching among different strategies. If $\lambda = 0$ the proportions do not change and are equal to 1/3, if $\lambda \to +\infty$ in each period each trader choose the strategy with the highest fitness. We assume the following fitness functions:

$$U_{i,t} = \log\left[\left(P_{i,t} - P_{i,t-1} - E_{i,t,t-1}\left[P_{i,t} - P_{i,t-1}\right]\right)^2\right] \tag{10}$$

The logarithm simplify with the exponential and therefore prevents the agents from switching too fast, indeed equation (9) simplify to:

$$n_{i,t} = \frac{\left(P_{i,t} - P_{i,t-1} - E_{i,t,t-1}\left[P_{i,t} - P_{i,t-1}\right]\right)^{-2\lambda}}{\sum_j \left(P_{j,t} - P_{j,t-1} - E_{j,t,t-1}\left[P_{j,t} - P_{j,t-1}\right]\right)^{-2\lambda}}$$

An exponential switching may provoke a speculative bubble when the trend followers monopolize the market and the price would converge to zero or diverge to infinity. The fitness function that we utilize rules out this possibility and does not require a penalty function as in Gaunersdorfer, Hommes and Wagener (2000).

The system may be made stationary by introducing the variables $M_t \equiv F_t - P_t$ and $\rho_t \equiv P_t - P_{t-1}$. In this way the system reads as:

$$\begin{aligned}
&\psi_{tf,t+1,t+2} = (1 - c_{tf})\psi_{tf,t,t+1} + c_{tf}\rho_{t+1};\ c_{tf} \in (0,1) \\
&\psi_{c,t+1,t+2} = (1 - c_c)\psi_{c,t,t+1} - c_c\rho_{t+1};\ c_c \in (0,1) \\
&M_{t+1} = M_t + \phi - \rho_{t+1} \\
&n_{i,t} = \frac{\exp\left[-\lambda \log\left[\left(\rho_t - E_{i,t,t+1}\left[P_{j,t+1} - P_{j,t}\right]\right)^2\right]\right]}{\sum_j \exp\left[-\lambda \log\left[\left(\rho_t - E_{j,t,t+1}\left[P_{j,t+1} - P_{j,t}\right]\right)^2\right]\right]}
\end{aligned} \tag{11}$$

where:

$$\xi_t = n_{f,t-1} a\left[M_{t-1} - \frac{g}{\eta}\right] + n_{tf,t-1}\gamma_{tf} \arctan\left[\theta_{tf}\left(\psi_{tf,t-1} - g\right)\right] + n_{c,t-1}\gamma_c \arctan\left[\theta_c\left(\psi_{c,t-1} - g\right)\right] -$$
$$\left(n_{f,t-2} a\left[M_{t-2} - \frac{g}{\eta}\right] + n_{tf,t-2}\gamma_{tf} \arctan\left[\theta_{tf}\left(\psi_{tf,t-2} - g\right)\right] + n_{c,t-2}\gamma_c \arctan\left[\theta_c\left(\psi_{c,t-2} - g\right)\right]\right) \quad (12)$$
$$\rho_t = \beta\xi_t + \alpha M_{t-1}$$

Equations (11) and *(12)* define a ten-dimensional difference equation system and imply the following the characterisation for the equilibrium:

Proposition 1. The system given by (11) and (12) has a fixed point such that : $\rho = E_{tf} = \phi = -E_c$, $n_f = n_c = 0$, $n_{tf} = 1$, $M = \phi/\alpha$ if and only if $\alpha \neq 0$.

Proof. If the system is on a fixed point, from the first two equations of (11) we get that $E_{tf} = -E_c = \rho$. The third equation implies that $\rho_t = \phi$. Since only the trend following strategy features a mean square error of zero, it follows from the equations governing the dynamics for n_i that $n_f = n_c = 0$ and $n_{tf} = 1$, i.e. only trend followers survive and monopolize the market. As a consequence, (12) implies that the excess demand ξ is zero and by replacing for ρ in the second equation of (12) we obtain $M = \phi/\alpha$.

Therefore at the fixed point the asset is mispriced but both the price and the fundamental value grows at the same rate. Since there are no fundamentalists on the market the stabilization of the price at the fundamental value happens because of the action of the market maker. Since the market maker take only into account the current difference between fundamental and price but not the growth rate of the fundamental, a mispricing remains that depends on the fundamental growth. Such mispricing may be easily eliminated by changing the behaviour of the market maker, therefore the fixed point may be considered as a fundamental state state.

Proposition 2. If $\lambda > 0.5$ and $\alpha + c_{tf}(1-\alpha) - \frac{c_{tf}\left(c_{tf} + \alpha\right)\beta\gamma_{tf}\theta_{tf}}{1 + \theta_{tf}^2\left(g - \phi\right)^2} > 0$ the fixed point is locally stable.

The fixed point undergoes a Neimark-Sacker bifurcation when $\alpha + c_{tf}(1-\alpha) - \left[c_{tf}\left(c_{tf} + \alpha\right)\beta\gamma_{tf}\theta_{tf} / \left(1 + \theta_{tf}^2\left(g - \phi\right)^2\right)\right] = 0$.

Proof: If we define the lagged variables $Z_{tf,t,t-1} = \psi_{tf,t-1,t-2}; Z_{c,t,t-1} = \psi_{tf,t-1,t-2}; v_{f,t} = n_{f,t-1}$; $v_{tf,t} = n_{tf,t-1}$; $L_t = M_{t-1}$, by substitution in the system given by *Equations (11)* and *(12)*, an equivalent a 10-dimension first order difference map is obtained, whose Jacobian matrix is:

$$J = \left(\frac{\partial \psi_{tf}'}{\partial \mathbf{K}} \quad \frac{\partial \psi_c'}{\partial \mathbf{K}} \quad \frac{\partial M'}{\partial \mathbf{K}} \quad \frac{\partial n_f'}{\partial \mathbf{K}} \quad \frac{\partial n_{tf}'}{\partial \mathbf{K}} \quad \frac{\partial Z_{tf}'}{\partial \mathbf{K}} \quad \frac{\partial Z_c'}{\partial \mathbf{K}} \quad \frac{\partial L'}{\partial \mathbf{K}} \quad \frac{\partial v_{tf}'}{\partial \mathbf{K}} \quad \frac{\partial v_c'}{\partial \mathbf{K}}\right)^T \quad (13)$$

where $\mathbf{K} = \left(\psi_{tf} \quad \psi_c \quad M \quad n_f \quad n_{tf} \quad Z_{tf} \quad Z_c \quad L \quad v_{tf} \quad v_c\right)^T$. At the fixed point $\psi_{tf} = Z_{tf}; \psi_c = Z_c; M = L; n_{tf} = v_{tf}; n_c = v_c$, therefore by replacing ψ_{tf} , ψ_c , *M, n_{tf}* and *n_c* and the lagged variables with their equilibrium values we obtain:

$$\frac{\partial \psi_{tf}{}'}{\partial \mathbf{K}}\left(\phi,-\phi,\frac{\phi}{\alpha},0,1,\phi,-\phi,\frac{\phi}{\alpha},0,1\right)=\begin{pmatrix} 1+c_{tf}\left(\dfrac{\beta\gamma_{tf}\theta_{tf}}{1+\theta_{tf}^2(g-\phi)^2}\right) \\ 0 \\ c_{tf}\alpha \\ c_{tf}\beta\left(a\left(\dfrac{a\phi}{\alpha}-\dfrac{ag}{\eta}+\gamma_c\arctan\left[\theta_c(g+\phi)\right]\right)\right) \\ c_{tf}\beta\left(\gamma_{tf}\arctan\left[\theta_{tf}(\phi-g)\right]+\gamma_c\arctan\left[\theta_c(\phi-g)\right]\right) \\ -\dfrac{c\beta\gamma_{tf}\theta_{tf}}{1+\theta_{tf}^2(g-\phi)^2} \\ 0 \\ 0 \\ -\dfrac{c_{tf}\beta\left(-ag+\dfrac{a\eta\phi}{\alpha}+\eta\gamma_c\arctan\left[\theta_c(g+\phi)\right]\right)}{\eta} \\ c_{tf}\beta\left(\gamma_{tf}\arctan\left[\theta_{tf}(g-\phi)\right]-\gamma_c\left[\theta_{tf}(g-\phi)\right]\right) \end{pmatrix}$$

$$\frac{\partial \psi_{c}{}'}{\partial \mathbf{K}}\left(\phi,-\phi,\frac{\phi}{\alpha},0,1,\phi,-\phi,\frac{\phi}{\alpha},0,1\right)=\begin{pmatrix} -\dfrac{c_c\beta\gamma_{tf}\theta}{1+\theta_{tf}^2(g-\phi)^2} \\ 1-c_c \\ -c_c\alpha \\ -\dfrac{c_c\beta\left(-ag+\dfrac{a\eta\phi}{\alpha}+\eta\gamma_c\arctan\left[\theta_c(g+\phi)\right]\right)}{\eta} \\ c_c\beta\left(\gamma_{tf}\arctan\left[\theta_{tf}(g-\phi)\right]-\gamma_c\arctan\left[\theta_c(\phi+g)\right]\right) \\ -\dfrac{c_c\beta\gamma_{tf}\theta_{tf}}{1+\theta_{tf}^2(g-\phi)^2} \\ 0 \\ 0 \\ -\dfrac{c_c\beta\left(-ag+\dfrac{a\eta\phi}{\alpha}+\eta\gamma_c\arctan\left[\theta_c(g+\phi)\right]\right)}{\eta} \\ c_{tf}\beta\left(\gamma_{tf}\arctan\left[\theta_{tf}(\phi-g)\right]+\gamma_c\left[\theta_c(g+\phi)\right]\right) \end{pmatrix}$$

$$\frac{\partial M'}{\partial \mathbf{K}}\left(\phi,-\phi,\frac{\phi}{\alpha},0,1,\phi,-\phi,\frac{\phi}{\alpha},0,1\right)=\begin{pmatrix} -\dfrac{\beta\gamma_{tf}\theta_{tf}}{1+\theta_{tf}^2(g-\phi)^2} \\ 0 \\ 1-\alpha \\ \beta\left(\dfrac{ag}{\eta}-\dfrac{a\phi}{\alpha}-\gamma_c \arctan[\theta_c(g+\phi)]\right) \\ \beta\left(\gamma_{tf}\arctan[\theta_{tf}(g-\phi)]-\gamma_c \arctan[\theta_c(g+\phi)]\right) \\ \dfrac{\beta\gamma_{tf}\theta_{tf}}{1+\theta_{tf}^2(g-\phi)^2} \\ 0 \\ 0 \\ \beta\left(-\dfrac{ag}{\eta}+\dfrac{a\phi}{\alpha}+\gamma_c \arctan[\theta_c(g+\phi)]\right) \\ \beta\left(\gamma_{tf}\arctan[\theta_{tf}(\phi-g)]-\gamma_c[\theta_c(g+\phi)]\right) \end{pmatrix}$$

$\frac{\partial n_f'}{\partial \mathbf{K}}$ and $\frac{\partial n_{tf}'}{\partial \mathbf{K}}$ are indeterminate at the fixed point, therefore in order to check for the stability and bifurcations it is needed to check the limit as the variables approach the equilibrium values. Let us define the functions $\vartheta_1(x,n_{tf},n_c)$ and $\vartheta_2(x,n_{tf},n_c)$ as the functions defined by $\frac{\partial n_f'}{\partial \mathbf{K}}$ and $\frac{\partial n_{tf}'}{\partial \mathbf{K}}$ where $x=(M\alpha-\phi)=(L\alpha-\phi)$. By replacing ψ_{tf}, ψ_c, M and the lagged variables with the equilibrium values ϕ, $-\phi$ and ϕ/α, a few algebraic manipulations imply that at the equilibrium $\vartheta_1(x,n_{tf},n_c)$ and $\vartheta_2(x,n_{tf},n_c)$ are respectively:

$$\left(\begin{array}{l}
\frac{2\left(x^2\right)^{-\lambda}\lambda\left(\left(-\phi+\frac{\eta\phi}{\alpha}\right)^2\right)^{-\lambda}\left(1+\frac{2^{-1-2\lambda}\,nc\,\alpha\beta\gamma1\theta tf\left(\phi^2\right)^{-\lambda}\left(2^{1+2\lambda}\phi\left(\phi^2\right)^{\lambda}\left(-\phi+\frac{\eta\phi}{\alpha}\right)+x\left(x^2\right)^{\lambda}\left(\phi+\frac{\eta\phi}{\alpha}\right)\right)}{(\alpha-\eta)\left(1+\theta tf^2(g-\phi)^2\right)\phi^2}\right)}{x\left(\left(x^2\right)^{-\lambda+4-\lambda}\left(\phi^2\right)^{-\lambda+}\left(\left(-\phi+\frac{\eta\phi}{\alpha}\right)^2\right)^{-\lambda}\right)^2} \\
\frac{2^{1-2\lambda}\left(x^2\right)^{-\lambda}\lambda\left(\phi^2\right)^{-\lambda}\left(\left(-\phi+\frac{\eta\phi}{\alpha}\right)^2\right)^{-\lambda}\left(-\frac{(-1+nc+ntf)\,\alpha\beta\gamma2\theta c\left(\left(x^2\right)^{\lambda}+4^{\lambda}\left(\phi^2\right)^{\lambda}\right)}{(-\alpha+\eta)\,\phi}-\right.}{\left.\frac{2^{1+2\lambda}(-1+nc+ntf)\,\beta\gamma2\theta c\phi\left(\phi^2\right)^{\lambda}+x\left(x^2\right)^{\lambda}\left(1+\theta c\left((-1+nc+ntf)\,\beta\gamma2+\theta c(g+\phi)^2\right)\right)}{2x\phi}\right)} \\
\frac{}{(1+\theta c^2(g+\phi)^2)\left(\left(x^2\right)^{-\lambda+4-\lambda}\left(\phi^2\right)^{-\lambda+}\left(\left(-\phi+\frac{\eta\phi}{\alpha}\right)^2\right)^{-\lambda}\right)^2} \\
\frac{2\alpha\lambda\left(\left(-\phi+\frac{\eta\phi}{\alpha}\right)^2\right)^{-\lambda}\left(\frac{\left(x^2\right)^{-\lambda}\left((-\alpha+\eta)\,\phi+a\,ntf\beta\left(-\phi+\frac{\eta\phi}{\alpha}\right)\right)}{x}+\frac{2^{-1-2\lambda}\left(\phi^2\right)^{-\lambda}\left((\alpha-\eta)\,\phi+a\,ntf\beta\left(\phi+\frac{\eta\phi}{\alpha}\right)\right)}{\phi}\right)}{(-\alpha+\eta)\,\phi\left(\left(x^2\right)^{-\lambda+4-\lambda}\left(\phi^2\right)^{-\lambda+}\left(\left(-\phi+\frac{\eta\phi}{\alpha}\right)^2\right)^{-\lambda}\right)^2} \\
\frac{4^{\lambda}\left(x^2\right)^{\lambda}\alpha\beta\lambda\left(\phi^2\right)^{\lambda}\left(\left(-\phi+\frac{\eta\phi}{\alpha}\right)^2\right)^{2\lambda}\left(2^{1+2\lambda}\phi\left(\phi^2\right)^{\lambda}\left(-\phi+\frac{\eta\phi}{\alpha}\right)+x\left(x^2\right)^{\lambda}\left(\phi+\frac{\eta\phi}{\alpha}\right)\right)\left(-ag+\frac{a\eta\phi}{\alpha}+\gamma2\eta\,\text{ArcTan}[\theta c(g+\phi)]\right)}{x\eta\,(-\alpha+\eta)\,\phi^2\left(4^{\lambda}\left(x^2\right)^{\lambda}\left(\phi^2\right)^{\lambda+}\left(\left(-\phi+\frac{\eta\phi}{\alpha}\right)^2\right)^{\lambda}\left(\left(x^2\right)^{\lambda+4^{\lambda}}\left(\phi^2\right)^{\lambda}\right)\right)^2} \\
\frac{4^{\lambda}\left(x^2\right)^{\lambda}\alpha\beta\lambda\left(\phi^2\right)^{\lambda}\left(\left(-\phi+\frac{\eta\phi}{\alpha}\right)^2\right)^{2\lambda}\left(2^{1+2\lambda}\phi\left(\phi^2\right)^{\lambda}\left(-\phi+\frac{\eta\phi}{\alpha}\right)+x\left(x^2\right)^{\lambda}\left(\phi+\frac{\eta\phi}{\alpha}\right)\right)\left(\gamma1\,\text{ArcTan}[\theta tf(-g+\phi)]+\gamma2\,\text{ArcTan}[\theta c(g+\phi)]\right)}{x(-\alpha+\eta)\,\phi^2\left(4^{\lambda}\left(x^2\right)^{\lambda}\left(\phi^2\right)^{\lambda+}\left(\left(-\phi+\frac{\eta\phi}{\alpha}\right)^2\right)^{\lambda}\left(\left(x^2\right)^{\lambda+4^{\lambda}}\left(\phi^2\right)^{\lambda}\right)\right)^2} \\
\frac{4^{\lambda}\,nc\left(x^2\right)^{\lambda}\alpha\beta\gamma1\theta tf\lambda\left(\phi^2\right)^{\lambda}\left(\left(-\phi+\frac{\eta\phi}{\alpha}\right)^2\right)^{2\lambda}\left(2^{1+2\lambda}\phi\left(\phi^2\right)^{\lambda}\left(\phi-\frac{\eta\phi}{\alpha}\right)+x\left(x^2\right)^{\lambda}\left(\phi+\frac{\eta\phi}{\alpha}\right)\right)}{x(-\alpha+\eta)\,\left(1+\theta tf^2(g-\phi)^2\right)\phi^2\left(4^{\lambda}\left(x^2\right)^{\lambda}\left(\phi^2\right)^{\lambda+}\left(\left(-\phi+\frac{\eta\phi}{\alpha}\right)^2\right)^{\lambda}\left(\left(x^2\right)^{\lambda+4^{\lambda}}\left(\phi^2\right)^{\lambda}\right)\right)^2} \\
\frac{2(1-nc-ntf)\,\alpha\beta\gamma2\theta c\lambda\left(\left(-\phi+\frac{\eta\phi}{\alpha}\right)^2\right)^{-\lambda}\left(\frac{\left(x^2\right)^{-\lambda}\left(-\phi+\frac{\eta\phi}{\alpha}\right)}{x}+\frac{2^{-1-2\lambda}\left(\phi^2\right)^{-\lambda}\left(\phi+\frac{\eta\phi}{\alpha}\right)}{\phi}\right)}{(\alpha-\eta)\,\phi\,(1+\theta c^2(g+\phi)^2)\left(\left(x^2\right)^{-\lambda+4-\lambda}\left(\phi^2\right)^{-\lambda+}\left(\left(-\phi+\frac{\eta\phi}{\alpha}\right)^2\right)^{-\lambda}\right)^2} \\
\frac{2\,ntf\alpha\beta\lambda\left(\left(-\phi+\frac{\eta\phi}{\alpha}\right)^2\right)^{-\lambda}\left(\frac{\left(x^2\right)^{-\lambda}\left(-\phi+\frac{\eta\phi}{\alpha}\right)}{x}+\frac{2^{-1-2\lambda}\left(\phi^2\right)^{-\lambda}\left(\phi+\frac{\eta\phi}{\alpha}\right)}{\phi}\right)}{(\alpha-\eta)\,\phi\left(\left(x^2\right)^{-\lambda+4-\lambda}\left(\phi^2\right)^{-\lambda+}\left(\left(-\phi+\frac{\eta\phi}{\alpha}\right)^2\right)^{-\lambda}\right)^2} \\
\frac{4^{\lambda}\left(x^2\right)^{\lambda}\alpha\beta\lambda\left(\phi^2\right)^{\lambda}\left(\left(-\phi+\frac{\eta\phi}{\alpha}\right)^2\right)^{2\lambda}\left(2^{1+2\lambda}\phi\left(\phi^2\right)^{\lambda}\left(\phi-\frac{\eta\phi}{\alpha}\right)+x\left(x^2\right)^{\lambda}\left(\phi+\frac{\eta\phi}{\alpha}\right)\right)\left(-ag+\frac{a\eta\phi}{\alpha}+\gamma2\eta\,\text{ArcTan}[\theta c(g+\phi)]\right)}{x\eta\,(-\alpha+\eta)\,\phi^2\left(4^{\lambda}\left(x^2\right)^{\lambda}\left(\phi^2\right)^{\lambda+}\left(\left(-\phi+\frac{\eta\phi}{\alpha}\right)^2\right)^{\lambda}\left(\left(x^2\right)^{\lambda+4^{\lambda}}\left(\phi^2\right)^{\lambda}\right)\right)^2} \\
\frac{4^{\lambda}\left(x^2\right)^{\lambda}\alpha\beta\lambda\left(\phi^2\right)^{\lambda}\left(\left(-\phi+\frac{\eta\phi}{\alpha}\right)^2\right)^{2\lambda}\left(2^{1+2\lambda}\phi\left(\phi^2\right)^{\lambda}\left(\phi-\frac{\eta\phi}{\alpha}\right)+x\left(x^2\right)^{\lambda}\left(\phi+\frac{\eta\phi}{\alpha}\right)\right)\left(\gamma1\,\text{ArcTan}[\theta tf(-g+\phi)]+\gamma2\,\text{ArcTan}[\theta c(g+\phi)]\right)}{x(-\alpha+\eta)\,\phi^2\left(4^{\lambda}\left(x^2\right)^{\lambda}\left(\phi^2\right)^{\lambda+}\left(\left(-\phi+\frac{\eta\phi}{\alpha}\right)^2\right)^{\lambda}\left(\left(x^2\right)^{\lambda+4^{\lambda}}\left(\phi^2\right)^{\lambda}\right)\right)^2}
\end{array}\right)$$

and:

$$\left(\frac{2(x^2)^{-\lambda}\lambda\left(4^{-\lambda}(\phi^2)^{-\lambda}+\left(\left(-\phi+\frac{\eta\phi}{\alpha}\right)^2\right)^{-\lambda}+\frac{4^{-\lambda}\,nc\beta\gamma1(-\alpha+\eta)\theta tf\phi(\phi^2)^{-\lambda}\left(\frac{(-\alpha+\eta)^2\phi^2}{\alpha^2}\right)^{-1-\lambda}\left(4^{\lambda}(\phi^2)^{\lambda}\left(-\phi+\frac{\eta\phi}{\alpha}\right)+\frac{(-\alpha+\eta)\phi\left(\left(-\phi+\frac{\eta\phi}{\alpha}\right)^2\right)^{\lambda}}{\alpha}\right)}{\alpha(1+\theta tf^2(g-\phi)^2)}\right)}{x\left((x^2)^{-\lambda}+4^{-\lambda}(\phi^2)^{-\lambda}+\left(\left(-\phi+\frac{\eta\phi}{\alpha}\right)^2\right)^{-\lambda}\right)^2}\right.$$

$$\frac{2(x^2)^{-\lambda}\lambda\left(\left(-\phi+\frac{\eta\phi}{\alpha}\right)^2\right)^{-\lambda}\left(\frac{(-1+nc+ntf)\alpha\beta\gamma2\theta c}{(-\alpha+\eta)\phi}+\frac{2^{-1-2\lambda}(\phi^2)^{-\lambda}\left(2^{1+2\lambda}(-1+nc+ntf)\beta\gamma2\theta c\phi(\phi^2)^{\lambda}+\left(\left(-\phi+\frac{\eta\phi}{\alpha}\right)^2\right)^{\lambda}(\phi+\theta c\phi(2(-1+nc+ntf)\beta\gamma2+\theta c(g+\phi)^2)-\phi(1+\theta c^2(g+\phi)^2))\right)}{x\phi}\right)}{(1+\theta c^2(g+\phi)^2)\left((x^2)^{-\lambda}+4^{-\lambda}(\phi^2)^{-\lambda}+\left(\left(-\phi+\frac{\eta\phi}{\alpha}\right)^2\right)^{-\lambda}\right)^2}$$

$$\frac{2(x^2)^{-\lambda}\lambda\left(4^{-\lambda(\alpha+a\,ntf\beta)}(\phi^2)^{-\lambda}+\frac{(-\alpha+\eta)\phi\left(\frac{(-\alpha+\eta)^2\phi^2}{\alpha^2}\right)^{-1-\lambda}\left((\alpha-\eta)\phi+a\,ntf\beta\left(\phi-\frac{\eta\phi}{\alpha}\right)\right)}{\alpha}\right)}{x\left((x^2)^{-\lambda}+4^{-\lambda}(\phi^2)^{-\lambda}+\left(\left(-\phi+\frac{\eta\phi}{\alpha}\right)^2\right)^{-\lambda}\right)^2}$$

$$\frac{2(x^2)^{-\lambda}\beta\lambda\left(4^{-\lambda}(\phi^2)^{-\lambda}+\frac{(-\alpha+\eta)\phi\left(\frac{(-\alpha+\eta)^2\phi^2}{\alpha^2}\right)^{-1-\lambda}\left(\phi-\frac{\eta\phi}{\alpha}\right)}{\alpha}\right)\left(a\left(-\frac{g}{\eta}+\frac{\phi}{\alpha}\right)+\gamma2\,\text{ArcTan}[\theta c(g+\phi)]\right)}{x\left((x^2)^{-\lambda}+4^{-\lambda}(\phi^2)^{-\lambda}+\left(\left(-\phi+\frac{\eta\phi}{\alpha}\right)^2\right)^{-\lambda}\right)^2}$$

$$\frac{2^{1+2\lambda}(x^2)^{\lambda}\alpha\beta\lambda(\phi^2)^{\lambda}\left(\left(-\phi+\frac{\eta\phi}{\alpha}\right)^2\right)^{\lambda}\left(4^{\lambda}(\phi^2)^{\lambda}\left(\phi-\frac{\eta\phi}{\alpha}\right)-\frac{(-\alpha+\eta)\phi\left(\left(-\phi+\frac{\eta\phi}{\alpha}\right)^2\right)^{\lambda}}{\alpha}\right)(\gamma1\,\text{ArcTan}[\theta tf(-g+\phi)]+\gamma2\,\text{ArcTan}[\theta c(g+\phi)])}{x(-\alpha+\eta)\phi\left(4^{\lambda}(x^2)^{\lambda}(\phi^2)^{\lambda}+\left(\left(-\phi+\frac{\eta\phi}{\alpha}\right)^2\right)^{\lambda}((x^2)^{\lambda}+4^{\lambda}(\phi^2)^{\lambda})\right)^2}$$

$$\frac{2^{1+2\lambda}nc(x^2)^{\lambda}\alpha\beta\gamma1\theta tf\lambda(\phi^2)^{\lambda}\left(\left(-\phi+\frac{\eta\phi}{\alpha}\right)^2\right)^{\lambda}\left(4^{\lambda}(\phi^2)^{\lambda}\left(-\phi+\frac{\eta\phi}{\alpha}\right)+\frac{(-\alpha+\eta)\phi\left(\left(-\phi+\frac{\eta\phi}{\alpha}\right)^2\right)^{\lambda}}{\alpha}\right)}{x(-\alpha+\eta)(1+\theta tf^2(g-\phi)^2)\phi\left(4^{\lambda}(x^2)^{\lambda}(\phi^2)^{\lambda}+\left(\left(-\phi+\frac{\eta\phi}{\alpha}\right)^2\right)^{\lambda}((x^2)^{\lambda}+4^{\lambda}(\phi^2)^{\lambda})\right)^2}$$

$$\frac{2(1-nc-ntf)(x^2)^{-\lambda}\beta\gamma2\theta c\lambda\left(\frac{\left(\frac{(-\alpha+\eta)^2\phi^2}{\alpha^2}\right)^{-\lambda}}{-\phi+\frac{\eta\phi}{\alpha}}+\frac{4^{-\lambda}(\phi^2)^{-\lambda}+\left(\left(-\phi+\frac{\eta\phi}{\alpha}\right)^2\right)^{-\lambda}}{x}\right)}{(1+\theta c^2(g+\phi)^2)\left((x^2)^{-\lambda}+4^{-\lambda}(\phi^2)^{-\lambda}+\left(\left(-\phi+\frac{\eta\phi}{\alpha}\right)^2\right)^{-\lambda}\right)^2}$$

$$\frac{2a\,ntf(x^2)^{-\lambda}\beta\lambda\left(\frac{\left(\frac{(-\alpha+\eta)^2\phi^2}{\alpha^2}\right)^{-\lambda}}{-\phi+\frac{\eta\phi}{\alpha}}+\frac{4^{-\lambda}(\phi^2)^{-\lambda}+\left(\left(-\phi+\frac{\eta\phi}{\alpha}\right)^2\right)^{-\lambda}}{x}\right)}{\left((x^2)^{-\lambda}+4^{-\lambda}(\phi^2)^{-\lambda}+\left(\left(-\phi+\frac{\eta\phi}{\alpha}\right)^2\right)^{-\lambda}\right)^2}$$

$$\frac{2(x^2)^{-\lambda}\beta\lambda\left(4^{-\lambda}(\phi^2)^{-\lambda}+\frac{(-\alpha+\eta)\phi\left(\frac{(-\alpha+\eta)^2\phi^2}{\alpha^2}\right)^{-1-\lambda}\left(\phi-\frac{\eta\phi}{\alpha}\right)}{\alpha}\right)\left(\frac{ag}{\eta}-\frac{a\phi}{\alpha}-\gamma2\,\text{ArcTan}[\theta c(g+\phi)]\right)}{x\left((x^2)^{-\lambda}+4^{-\lambda}(\phi^2)^{-\lambda}+\left(\left(-\phi+\frac{\eta\phi}{\alpha}\right)^2\right)^{-\lambda}\right)^2}$$

$$\left.\frac{2^{1+2\lambda}(x^2)^{\lambda}\alpha\beta\lambda(\phi^2)^{\lambda}\left(\left(-\phi+\frac{\eta\phi}{\alpha}\right)^2\right)^{\lambda}\left(4^{\lambda}(\phi^2)^{\lambda}\left(-\phi+\frac{\eta\phi}{\alpha}\right)+\frac{(-\alpha+\eta)\phi\left(\left(-\phi+\frac{\eta\phi}{\alpha}\right)^2\right)^{\lambda}}{\alpha}\right)(\gamma1\,\text{ArcTan}[\theta tf(-g+\phi)]+\gamma2\,\text{ArcTan}[\theta c(g+\phi)])}{x(-\alpha+\eta)\phi\left(4^{\lambda}(x^2)^{\lambda}(\phi^2)^{\lambda}+\left(\left(-\phi+\frac{\eta\phi}{\alpha}\right)^2\right)^{\lambda}((x^2)^{\lambda}+4^{\lambda}(\phi^2)^{\lambda})\right)^2}\right)$$

The degrees of the functions at the numerators and denominators of each component of $\frac{\partial n_f'}{\partial \mathbf{K}}$ and $\frac{\partial n_{tf}'}{\partial \mathbf{K}}$ imply that if $\lambda > 0.5$, $\alpha \neq \eta$,

$$\lim\left[\begin{pmatrix}\vartheta_1\left(x, n_{tf}, n_c\right)\\ \vartheta_2\left(x, n_{tf}, n_c\right)\end{pmatrix}, x \to 0, n_{tf} \to 1, n_c \to 0\right] = 0 \tag{14}$$

If $\lambda < 0.5$ the limit does not exit and if $\lambda = 0.5$ the limit tends to a finite value. The last five rows of the jacobian matrix are:

$$\begin{pmatrix}\frac{\partial \varepsilon_{tf}'}{\partial \mathbf{K}} & \frac{\partial \varepsilon_c'}{\partial \mathbf{K}} & \frac{\partial L'}{\partial \mathbf{K}} & \frac{\partial v_{tf}'}{\partial \mathbf{K}} & \frac{\partial v_c'}{\partial \mathbf{K}}\end{pmatrix}^T = \begin{pmatrix}1&0&0&0&0&0&0&0&0&0\\0&1&0&0&0&0&0&0&0&0\\0&0&1&0&0&0&0&0&0&0\\0&0&0&1&0&0&0&0&0&0\\0&0&0&0&1&0&0&0&0&0\end{pmatrix} \tag{15}$$

It follows from the structure of the Jacobian matrix that six eigenvalues are zero, while the remaining four are equal of those of the following matrix:

$$\begin{pmatrix}1+c_{tf}\left(\frac{\beta\gamma_{tf}\theta_{tf}}{1+\theta_{tf}^2(g-\phi)^2}-1\right) & 0 & c\alpha & -\frac{c_{tf}\beta\gamma_{tf}\theta_{tf}}{1+\theta_{tf}^2(g-\phi)^2}\\ -\frac{c_c\beta\gamma_{tf}\theta_{tf}}{1+\theta_{tf}^2(g-\phi)^2} & 1-c_c & -c_{c\alpha} & \frac{c_c\beta\gamma_{tf}\theta_{tf}}{1+\theta_{tf}^2(g-\phi)^2}\\ -\frac{\beta\gamma_{tf}\theta_{tf}}{1+\theta_{tf}^2(g-\phi)^2} & 0 & 1-\alpha & \frac{\beta\gamma_{tf}\theta_{tf}}{1+\theta_{tf}^2(g-\phi)^2}\\ 1 & 0 & 0 & 0\end{pmatrix} \tag{16}$$

One eigenvalue is $\mu = 1 - c_c$, thus is always inside the unit circle and the manifold tangent to the associated eigenvector is stable. As a consequence, the equilibrium is locally stable if the eigenvalues of the following matrix are also inside the unit circle:

$$Q = \begin{pmatrix}1+c_{tf}\left(\frac{\beta\gamma_{tf}\theta_{tf}}{1+\theta_{tf}^2(g-\phi)^2}-1\right) & c\alpha & -\frac{c_{tf}\beta\gamma_{tf}\theta_{tf}}{1+\theta_{tf}^2(g-\phi)^2}\\ -\frac{\beta\gamma_{tf}\theta_{tf}}{1+\theta_{tf}^2(g-\phi)^2} & 1-\alpha & \frac{\beta\gamma_{tf}\theta_{tf}}{1+\theta_{tf}^2(g-\phi)^2}\\ 1 & 0 & 0\end{pmatrix} \tag{17}$$

The characteristic equation of Q is $\Gamma(Q) = \xi^3 + p_1\xi^2 + p_2\xi + p3 = 0$, where $p_1 = trace(Q)$; p_2 is defined as the sum of the principal minor of Q and $p_3 = \det(Q)$. Sonis (2000) proves that a necessary and sufficient condition for stability is $\Delta_1, \Delta_2, \Delta_3 > 0$ where:

$$\Delta_1 = 1 + p_1 + p_2 + p_3 = c_{tf}\alpha$$
$$\Delta_2 = 1 - p_1 + p_2 - p_3 = (c_{tf} - 2)(\alpha - 2) + \frac{2c_{tf}\beta\gamma_{tf}\theta_{tf}}{1 + \theta_{tf}(g - \phi)^2} \tag{18}$$
$$\Delta_3 = 1 - p_2 + p_3(p_1 - p_3) = \alpha + c_{tf}(1 - \alpha) - \frac{c_{tf}(c_{tf} + \alpha)\beta\gamma_{tf}\theta_{tf}}{1 + \theta_{tf}^2(g - \phi)^2}$$

If $\Delta_1 = 0$ two eigenvalues lies inside the unit circle and the third is $\mu = 1$; therefore the fixed point undergoes a fold bifurcation; if $\Delta_2 = 0$ two eigenvalues lies inside the unit circle and the third is $\mu = -1$; therefore the fixed point undergoes a flip (period doubling) bifurcation; if $\Delta_3 = 0$ one eigenvalue lies inside the unit circle and the remaining two satisfy $\mu_{2,3} = e^{2\pi i\vartheta}$. $\Delta_1, \Delta_2 > 0$ for any feasible parameter values, thus the fixed point may lose the stability only with a Neimark-Sacker bifurcation. Q.E.D.

The functional form of Δ_3 implies the following:

1) The price adjustment that the market maker performs in order to prevent the mispricing from becoming too large may be actually destabilizing if $c_{tf}\beta\gamma_{tf}\theta_{tf} / \left(1 + \theta_{tf}^2(g - \phi)^2\right) > 1$, that is, if trend followers are not very risk averse, extrapolate strongly, the market maker is highly reactive to excess demand or if the difference between the rates of interest and growth is low. Indeed, the price adjustment from the maker toward the fundamental may trigger a strong reaction from the trend followers if they are highly reactive. This in turn brings about a strong price effect is the market maker is characterised by a high value of β. If the fundamental growth rate is close to the interest rate, the demand for the risky asset is low and this tend to stabilize the price.

2) The stability depends does not depend on the behavioural parameters of fundamentalists and contrarians, however these parameters affects the size of the stability region and the global dynamics as will be shown through numerical simulations. The local stability is not affected by the parameters governing the dynamics of the fundamentalists and contrarians because these agents disappear from the market when the system is at the equilibrium, however the trend followers must trade as fundamentalists for the system to remain at the equilibrium. Therefore the equilibrium becomes unstable if trend following trading is so strong as to give rise to large departure from the fundamental price.

3) In a stock based market, i.e. a market where the agents does not take into account current holdings and the market demand would be only given by the first order terms of the RHS of *Equation (6)*, the Neimark-Sacker condition is given by $\alpha + c_{tf}(1 - \alpha) - c_{tf}\beta\gamma_{tf}\theta_{tf} / \left(1 + \theta_{tf}^2(g - \phi)^2\right) = 0$, therefore if $(c_{tf} + \alpha) \in (0,1)$ a flow-based market is stable for a wider range of parameters. The converse happens if $(c_{tf} + \alpha) \in (1,2)$.

2.2 Analysis of bifurcations and global dynamics

We consider two different baseline model, with parameters reported in *Table1*. Those models have been examined by performed a numerical analysis of global dynamics and stochastic simulation by adding noises to the systems, as explained in the following section. *Table2* reports the initial value of the system variables employed in the simulations.

	α	β	g	γ_{tf}	γ_{tc}	θ_{tf}	θ_c	c_{tf}	c_c	a	η	ϕ	λ
System1	0.0005	0.005	0.00025	70	70	10	10	0.3	0.2	46	0.01	0.0002	2.8
System2	0.0005	0.0055	0.00025	1400	600	1.4	3.6	0.3	0.25	45	0.006	0.0002	0.15

Table 1:parameters values of *System1* and *System2*.

	$\psi_{tf}(0)$	$\psi_c(0)$	$Z_{tf}(0)$	$Z_c(0)$	n_f	n_{tf}	v_f	v_c
	0.01	0	0	0	0	1/3	0	1/3

Table 2: initial values of system variables in numerical simulations.

System 1 and *System2* differ basically for the speeds of prediction rule switching and technical trading reactions. The parameters have been selected as to give place to simulated time series similar to those generated by real markets on a daily time scale. The selected values for the interest and growth rates imply annual rates equal to g=6.44% and $\phi = 5.12\%$ if a year is assumed to be composed of 250 trading days. The fundamentalists assume that on average a mispricing is reduced in a daily time unit by about 1% in *System1* and 0.6% in *System2*. The selected values of a and η determine the relations between risk and expected return represented in *Figure 1*.

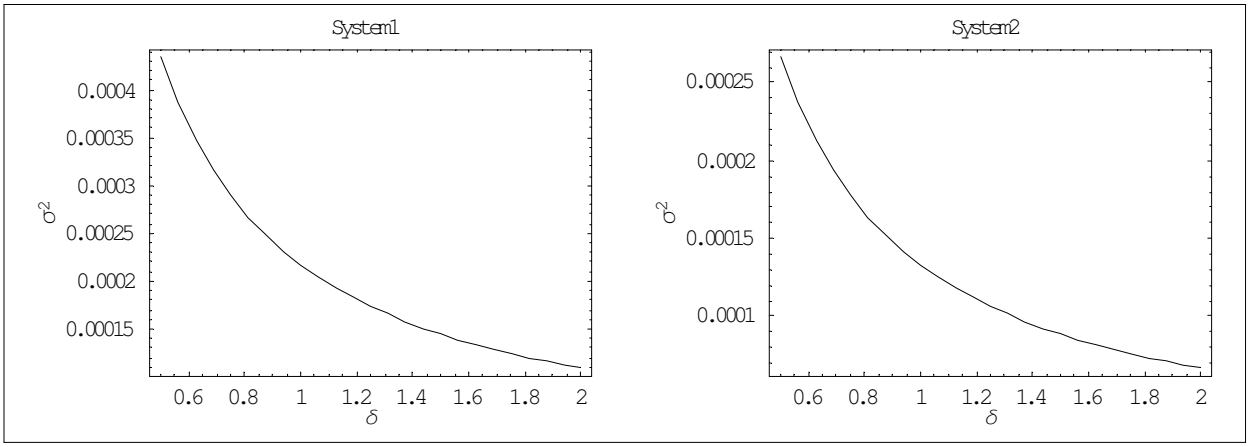

Figure 1: Relations between expected return and risk aversion of fundamentalists for *System1* and *System2*.

As far as the behaviour of the technical traders is concerned, while in *System1* they behave in symmetrical way, except for the extrapolation speed that is slightly higher for trend followers, in *System2* the difference between γ_{tf} and γ_c is almost completely offset by the difference between in θ_{tc} and θ_c. Indeed, as shown in *Figure2*, the absolute value of optimal demands of trend followers and contrarians are very similar, with contrarians a little risk averse for expected return within the interval [-0.1777,-0.1782]. The values of α has been chosen quite small with respect to β, because we assume that the price changes are mainly driven by the trading of the investors and the role of the market maker consists substantially of clearing the market with the reduction of the mispricing only a residual function.

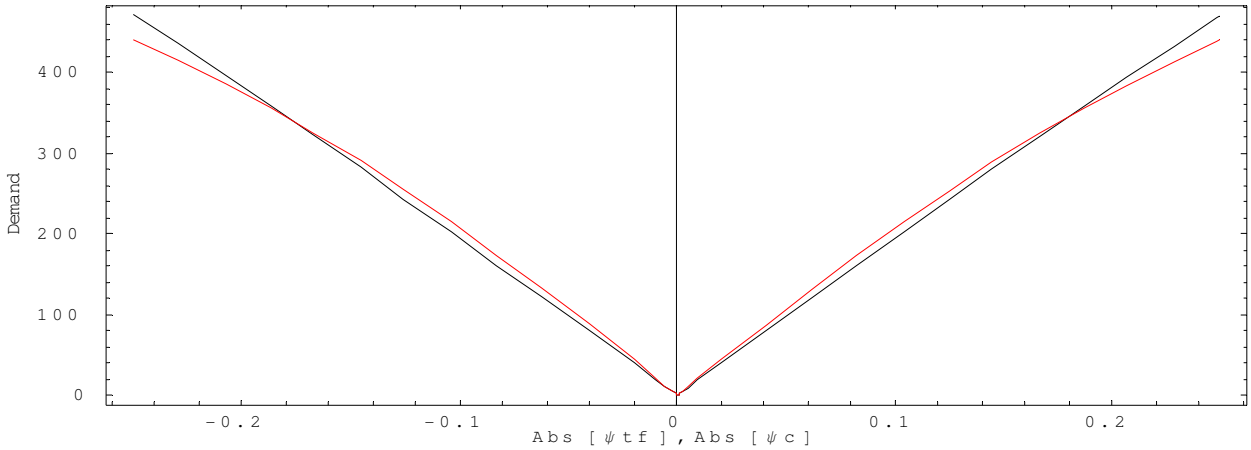

Figure 2: The absolute value of the demands of trend followers (black) and contrarians (red) as ψ_{tf} and ψ_c vary between -0.25 and 0.25.

System1 is characterised by a strange attractor and a strange repeller at the selected parameter values. The convergence to the attractor may be very slow and the speed of convergence is highly dependent on initial conditions. The attractor features very small proportions of fundamentalists and ψ_{tc},ψ_c are very close to zero. In *Figure 3* are represented the time series of the last 20000 observations, obtained after a transient phase of 10000 iterations, of $\psi_{tc},\psi_c,n_f,n_{tf}$ and the projections on planes (ψ_{tf},ψ_c) and (n_f,n_{tf}). In *Figure 4* are displayed the time series and projection for $C_{tf}=0.7$ and $c_c=0.2$, the system converges to a strange attractor very similar to the repeller of left panel of *Figure 3* but features a very high expected return variance. and The left Panel displays the dynamics with the initial values reported in *Table 2*, the right Panel has instead been obtained changing the initial expected returns and proportions to $n_f(0)=v_f(0)=0.3275$ and $n_{tf}(0)=v_{tf}(0)=0.3725$. It is apparent that in the first case the system is still close to the chaotic repeller. *Figure 5* displays on planes (n_f,n_{tf}) (left panel) and (ψ_{tf},ψ_c) (right panel) the sets of values $n_f(0)=v_f(0),n_{tf}(0)=v_{tf}(0)$ and $\psi_{tf,1,0}$, $\psi_{c,1,0}$ such that the system is still close to the repeller after 20000 iterations (in dark grey) and the set of values $\psi_{tf,1,0}$, $\psi_{c,1,0}$ and of $n_f(0)=v_f(0),n_{tf}(0)=v_{tf}(0)$ (in light grey) such that the system has already converged to the attractor after 20000 iterations. The white triangle in the left planes identify initial proportions of fundamentalists and trend followers that are not feasible because otherwise the proportion of contrarians would be negative.

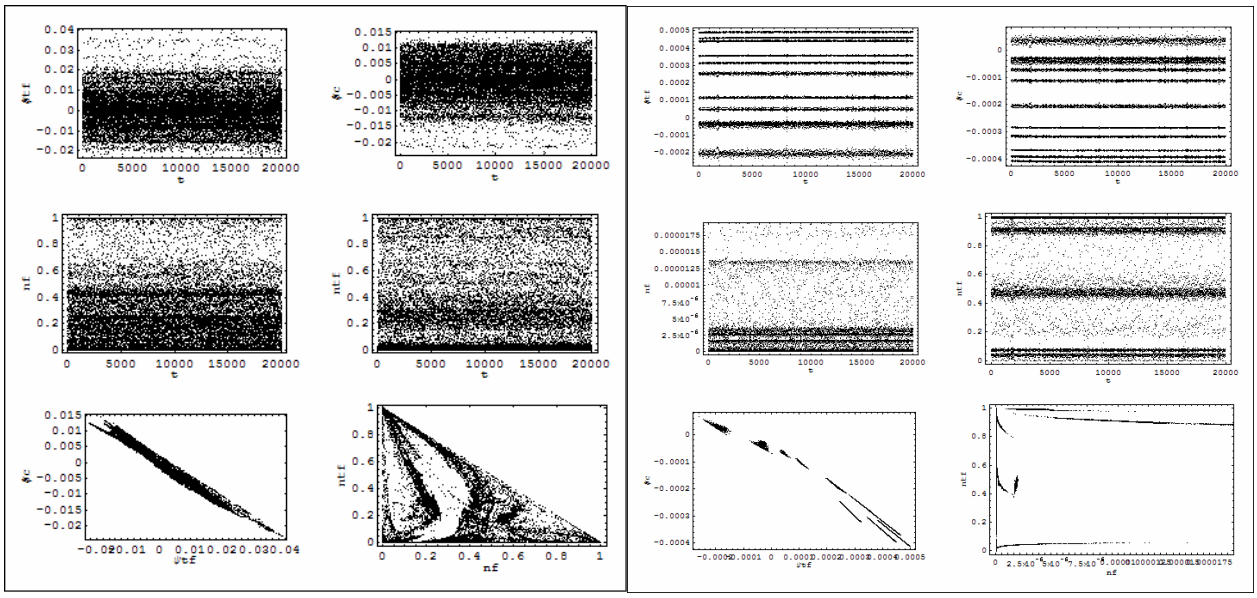

Figure 3: Time series of expected returns of trend followers and contrarians, proportions of fundamentalists and trend followers, projections of the time series on planes (ψ_{tf}, ψ_c) and (n_f, n_{tf}) of *System1* with baseline initial values (left panel) and $n_f(0) = v_f(0) = 0.3275$ and $n_{tf}(0) = v_{tf}(0) = 0.3725$ (right panel).

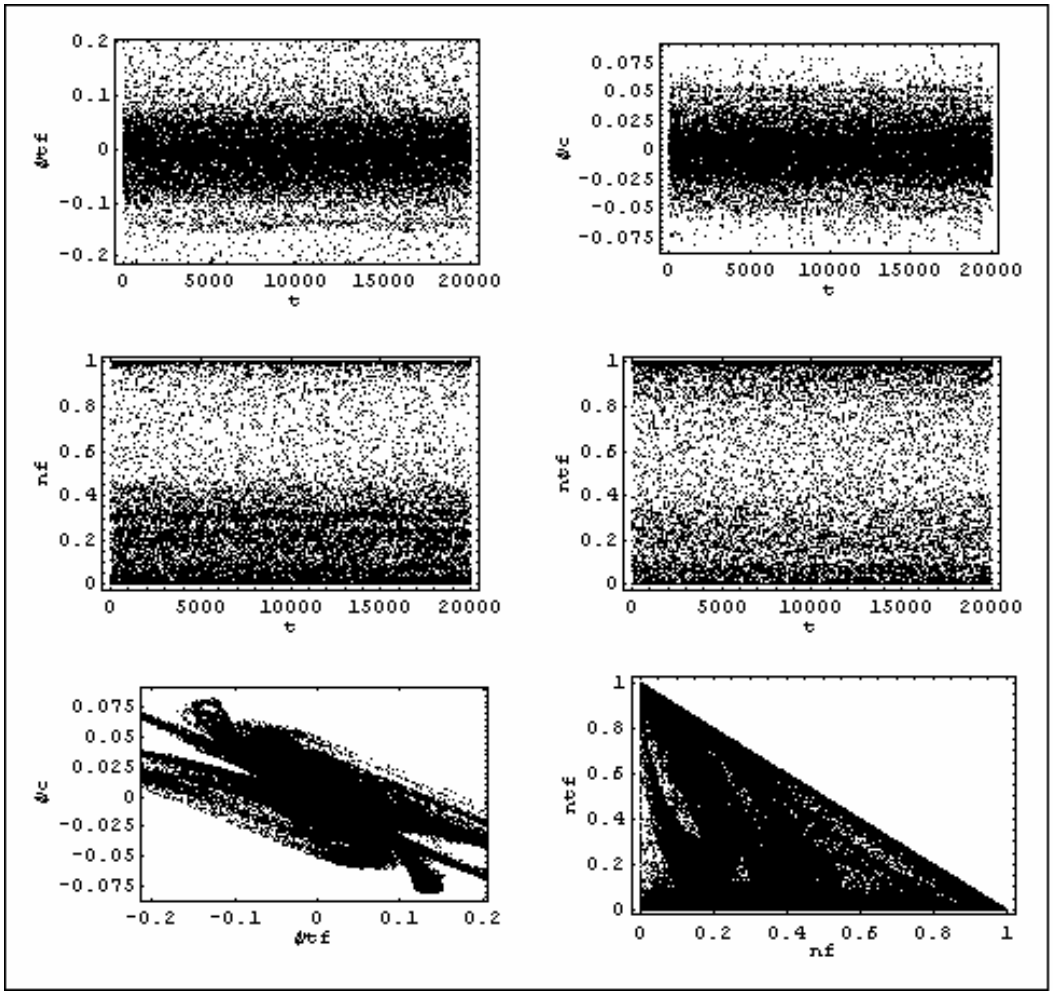

Figure 4: Time series of expected returns of trend followers and contrarians, proportions of fundamentalists and trend followers, projections of the time series on planes (ψ_{tf}, ψ_c) and (n_f, n_{tf}) of *System1* with c_{tf}=0.7 and c_c=0.2

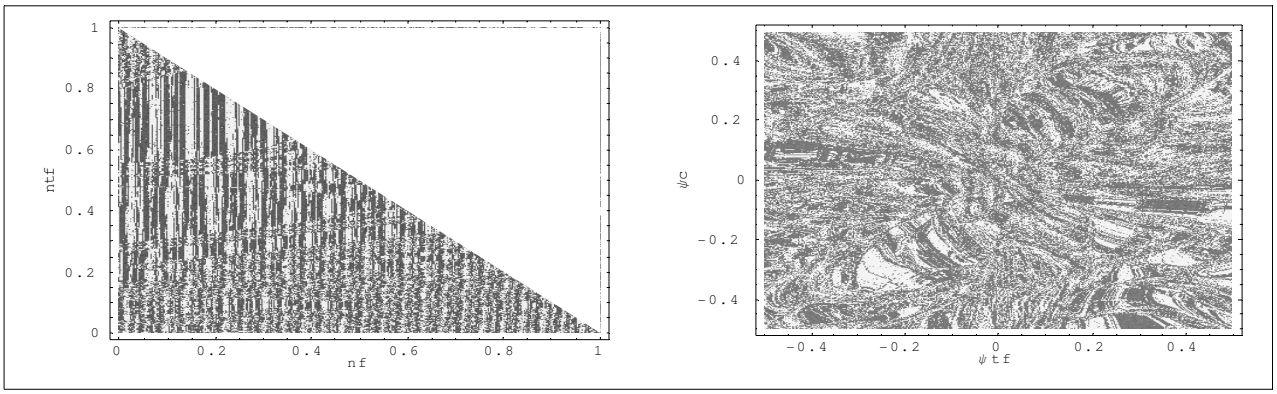

Figure 5: Sets of values $n_f(0) = v_f(0), n_{tf}(0) = v_{tf}(0)$ (left panel) and $\psi_{tf,1,0}$, $\psi_{c,1,0}$ (right panel) such that the system is still close to the repeller after 20000 iterations (in dark grey) and the set of values $\psi_{tf,1,0}$, $\psi_{c,1,0}$ and of $n_f(0) = v_f(0), n_{tf}(0) = v_{tf}(0)$ (in light grey) such that the system has already converged to the attractor after 20000 iterations.

Figure 6 reports the 2-parameters bifurcation diagrams on the parameter spaces $(c_{tf}, c_c); (a, \eta); (\gamma_{tf}, \gamma_c); (g, \phi); (\theta_1, \theta_2); (\alpha, \beta); (\gamma_{tf}, \theta_{tf})$, which have been obtained by iterating the system up to 1000 iterations after transient of 20000 and reports 1,2,3,4,5,6,7,8-period cycles in different colours, the area associated to higher period cycle, quasi-periodic or chaotic attractors are drawn in a grey scale with lighter colours associated to a larger number of different values of ψ_{tf}. Two values are assumed to be different if their percentage difference is less than 0.001. The areas where the price diverges are plotted in yellow. The big points identify the parameter values of baseline model and the small one identify parameter values for which we calculated the autocorrelograms reported in *Figure 16-19.* The Neimark-Sacker curve is plotted white if it is inside the range of simulated parameter values. It can be checked by calculating the value of Δ_3 that the baseline model is outside the stability region. The presence of other attractors than the fixed point within the Neimark-Sacker boundary makes it apparent that the system is characterised by coexistence of attractors. The importance of such phenomenon in determining calm and turbulent market phases with the associated volatility clustering has been pointed out by Hommes (1998) where a model is presented such that due to the degeneracy of the Neimark-Sacker bifurcation that gives place to a Chenciner bifurcation, which imply the co-existence of stable fixed point surrounded by a stable invariant curve. In our model, a stable fixed point co-exist with a periodic, aperiodic cycles and strange attractors. The basin of attraction of the fixed point tends to be very small and shows a Cantor structure as denoted by the magnification of parameter space $(\gamma_{tf}, \theta_{tf})$ reported in *Figure 7*, indeed it is very likely that the systems switches among different basins when buffeted with stochastic noise. Low values of the fundamental growth rate with respect to the interest rate determine the convergence toward a period-2 cycle. It is assumed that $\phi < g$ because otherwise the fundamental value would be infinite, if the fundamental is defined as the discount value of the dividend stream increasing at a rate ϕ. It is apparent from the 2-bifurcation diagrams (θ_{tf}, θ_c) and (γ_{tf}, γ_c) that $\gamma_{tf,c}$ nd $c_{tf,c}$ have similar effects on the asymptotic dynamics, in fact the system is likely to converge to the fixed point with low values of such parameters and to cycles or a strange attractor if the parameters are increased. The basin of attraction of the fixed point is wider if γ_{tf} or θ_{tf} have respectively the similar magnitude of γ_c or θ_c, and in some cases the simulations converges to the fixed point for parameter values up to the Neimark-Sacker boundary. Therefore if technical traders are not so reactive as to destabilise the equilibrium, contrarians may perform a stabilizing action because offset the trend followers. Therefore, even if the Neimark-Sacker bifurcation does not depend on the behavioural parameters of contrarians, a global analysis points out that a model with contrarians may be more stable than a model with only trend followers because the former affect the size of the basin of attraction of the fixed point. Higher values of the

reaction speeds of contrarians have on the other hand a destabilizing effect because tend to bring about too large price corrections. Very high contrarians' reactions break down the attractor into a 2-period cycle. The same is true as far as the speeds of expected return updating c_t, , c_c are concerned. The 1-parameter bifurcation diagrams shown in Figure 11 denotes that high values of γ_{tf} , θ_{tf} and c_1 change the scale of the system, that is, the asymptotic dynamics show converge toward attractors having a large volume. The 1-parameter bifurcation diagrams denote that an increase in the size of the attractor is related to the reaction speed of trend followers, therefore if a threshold value is passed, trend following trading may determine a turbulent phase with high volatility, and this threshold is directly dependent on contrarian trading. The time series and 2-dimensional phase space projection for $c_{tf} = 0.7$ and $c_c = 0.2$ are represented in *Figure 4*. The similarities with the repeller depicted in the left panel of *Figure 3* are appartent, however the volume of the attractor is larger and the variance of expected returns is higher. The fact that γ_{tf} and θ_{tf} show the same behaviour in determining the stability of the system is denoted from the bifurcation diagram of $(\gamma_{tf}, \theta_{tf})$ where the convergence toward the fixed point and periodic cycle has a pattern resembling the Neimark-Sacker boundary and an high value of θ_{tf} must be associated to a low value of γ_{tf} in order to preserve the stability. The set of parameters such that the system converge to the equilibrium is not connected, therefore it always co-exists with other attractors. Fundamentalists does not perform a stabilizing action either. Indeed a higher value of a and η does not stabilize the system and may instead destabilize it. Very high values of the expected mispricing correction and low values of fundamentalist risk aversion and/or expected variance will give rise to price divergence. This is due to the overreaction and price overshooting, which in turn trigger a strong response from trend followers. This phenomenon is also apparent from the 2-parameter bifurcation diagrams (a, η). In a discrete time model, price overshooting may is more likely to occur than in a continuous-time even if trend following trading is weak. While in the model dealt with in the previous chapter, fundamentalists may overshoot the fundamental value because of information processing delays, in this model a strong fundamentalist trading may make to price jump to a value higher (lower) than fundamental, if the asset were initially underpriced (overpriced). The bifurcation diagram of (α, β) denotes a chaotic window for intermediate values of β. α can stabilize the system only for low values of β because a high value of price sensitivity to excess demand trigger a strong response from the investors.

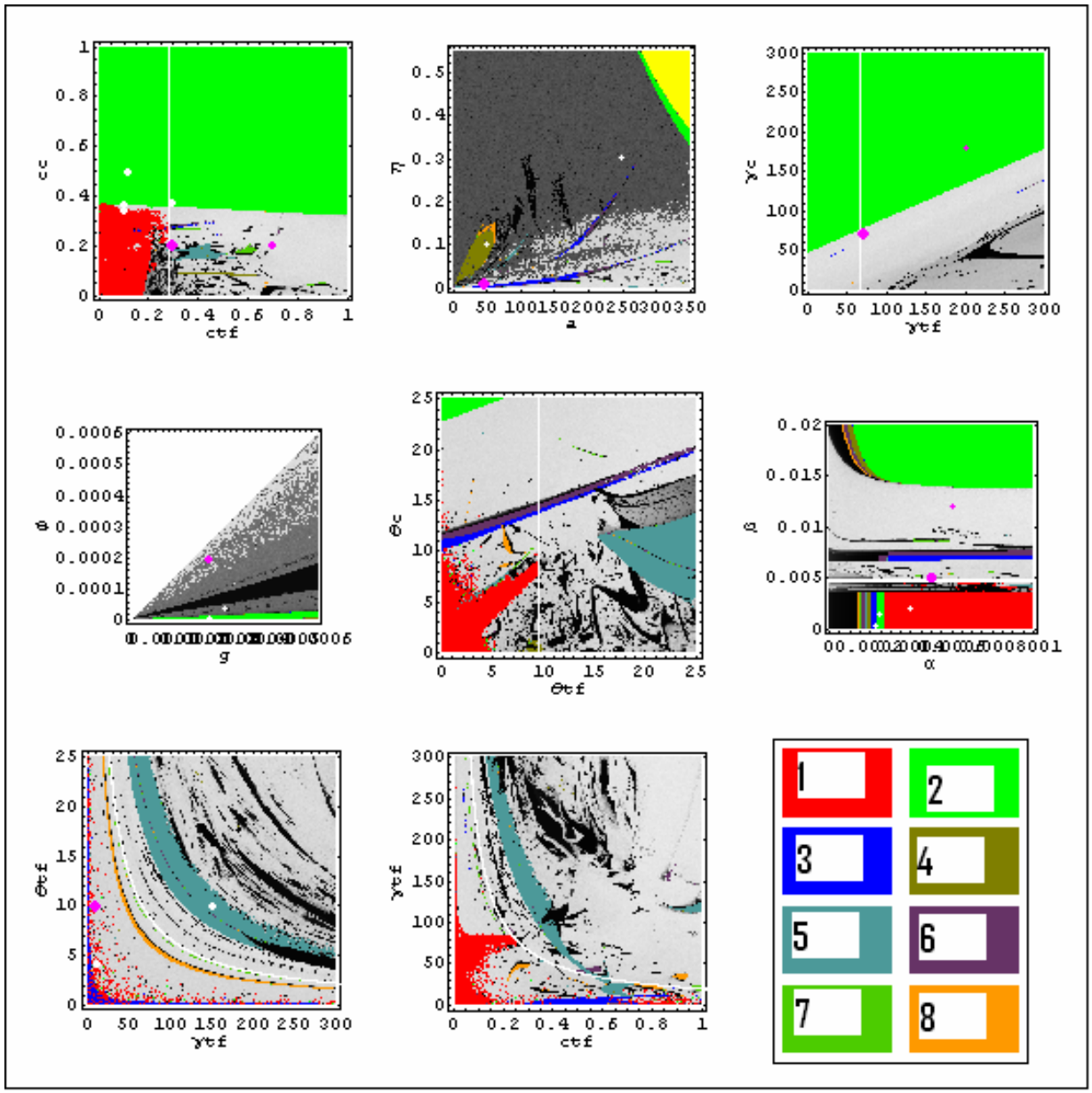

Figure 6: 2-parameter bifurcation diagrams of parameters $(c_{tf}, c_c); (a, \eta); (\gamma_{tf}, \gamma_c); (g, \phi); (\theta_1, \theta_2); (\alpha, \beta); (\gamma_{tf}, \theta_{tf}); (c_{tf}, \gamma_{tf})$ of *System1*. The panel at the right bottom display the colours associated to cycle periodicity.

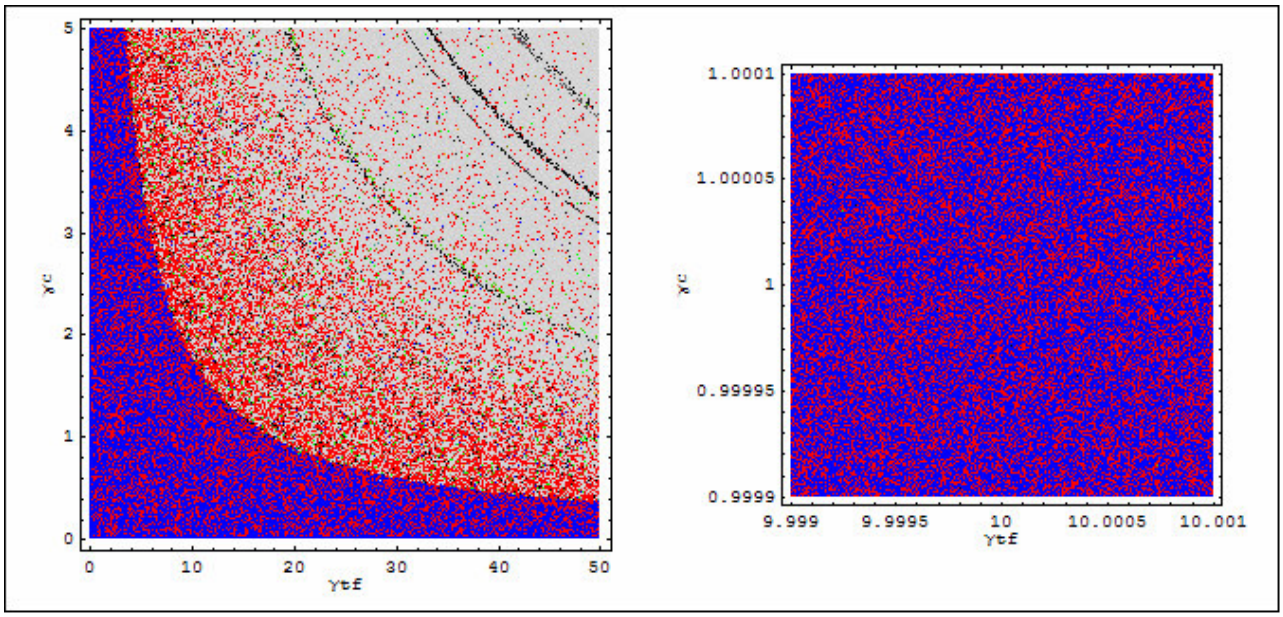

Figure 7: magnification of the bifurcation diagram $(\gamma_{tf}, \theta_{tf})$. The Cantor structure is apparent.

In Figure 8 there are represented the time series of the last 20000 observations, obtained after a transient phase of 10000 iterations, of $\psi_{tc}, \psi_c, n_f, n_{tf}$ and the projections on planes (ψ_{tf}, ψ_c) and (n_f, n_{tf}) of *System2*. With these parameter values, the model does not show the co-existence of chaotic repellers and chaotic attractors.

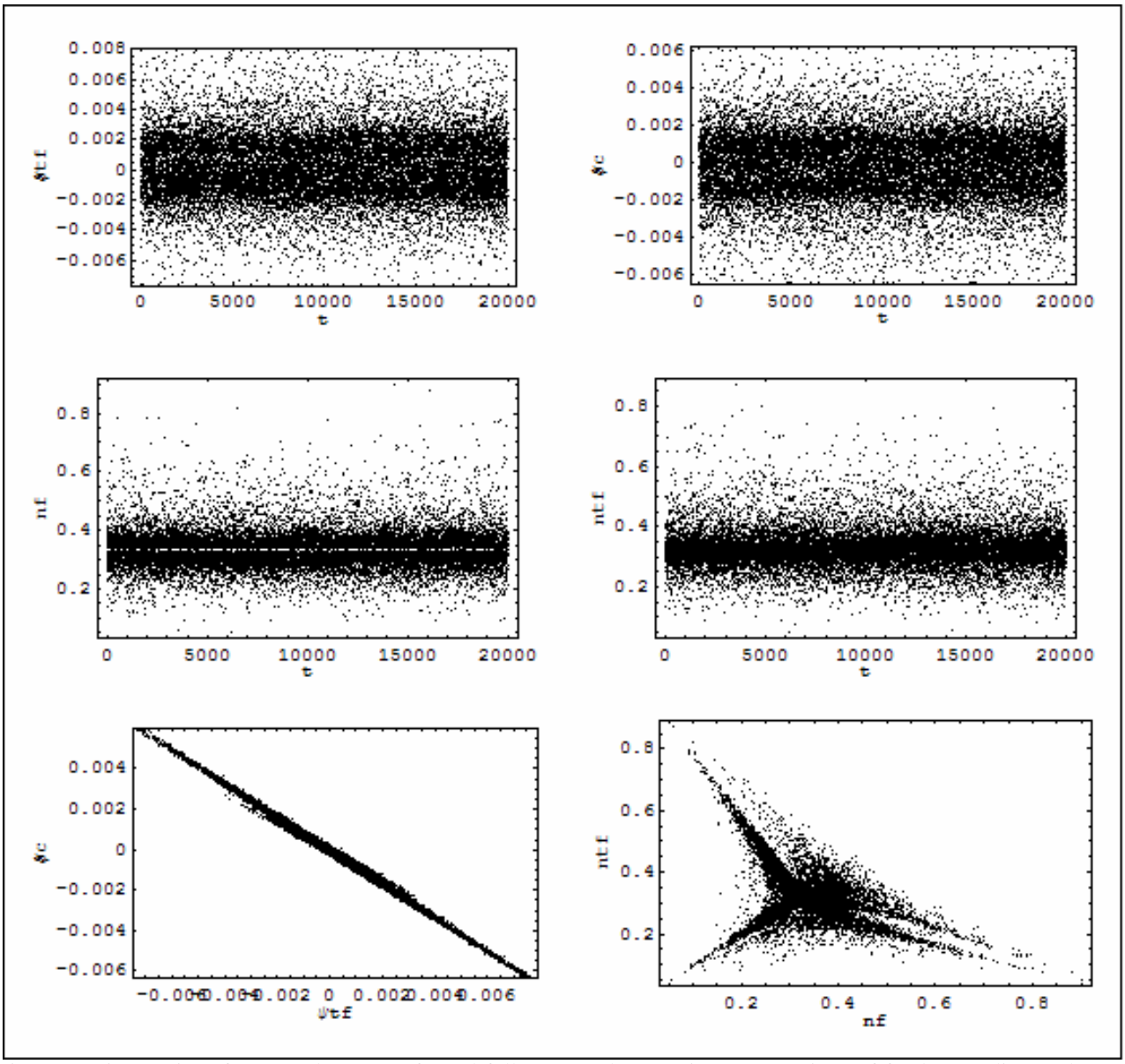

Figure 8: Time series of expected returns of trend followers and contrarians, proportions of fundamentalists and trend followers, projections of the time series on planes (ψ_{tf}, ψ_c) and (n_f, n_{tf}) of *System2* with baseline initial values.

An analysis of the bifurcation diagrams points out the following difference in the dynamics between *System1* and *System2*:

1) In *System2* c_c gives place to an oscillatory dynamics only for an interval of values, that is, there must be a balance between extrapolation speeds of trend followers and contrarians, a low risk aversion and/or low expected variance of contrarians determine a strong demand from these investors with high pricing switching and disorder in the system. If trend followers extrapolate strongly, contrarians are no longer able to offset trend followers and therefore the periodicity window disappear.

2) The bifurcation diagram (a, η) has a much simpler structure with only three periodicity band and does not show any patter toward any kind of stabilization. The fundamentalists were not able to render the system more tidy in *System1* and this behaviour is reinforced in the present case because of the stronger reactivity of technical traders due to higher values of $\gamma_{tf}, \gamma_c, \theta_{tc}, \theta_c$.

3) High values of γ_{tf} and/or θ_{tf} determine an increase in the volume of the attractor and a change in the shape, unless they are associated to high values of of γ_c and/or θ_c. In fact, the bifurcations diagrams displays a band with intermediate values of γ_{tf} (θ_{tf}) and γ_c (θ_c) where the system converges to the baseline chaotic attractor. In *Figure 9* are represented the time series of $\psi_{tc}, \psi_c, n_f, n_{tf}$ and the projections on planes (ψ_{tf}, ψ_c) and (n_f, n_{tf}) with $\gamma = 2000$ $\gamma_c = 100$. *Figure 10* illustrates the case of convergence to 2 chaotic bands that occurs when contrarians update the expected return much faster than trend followers, in fact $c_{tf} = 0.2$ and $c_c = 0.9$.

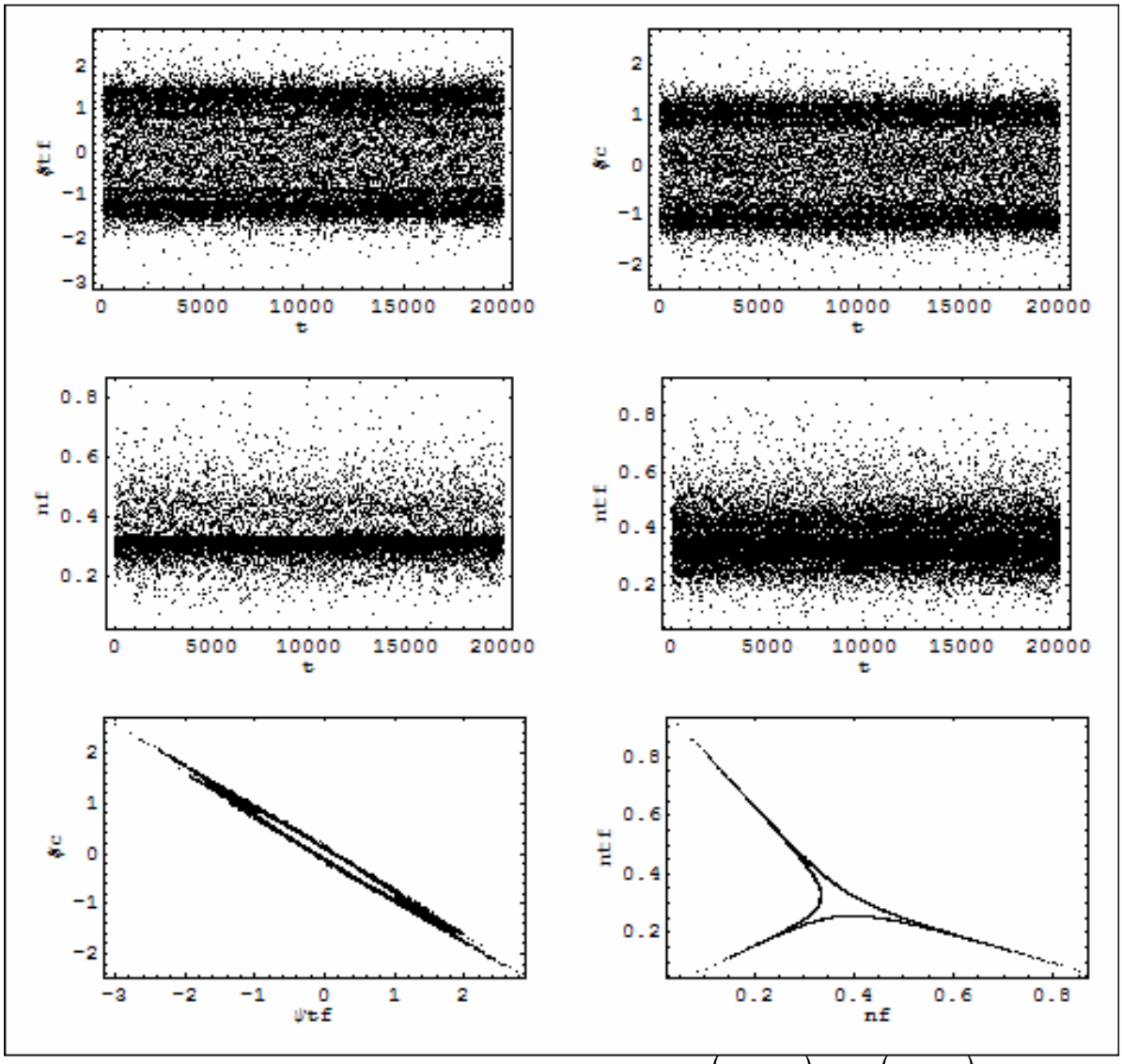

Figure 9: Time series of $\psi_{tc}, \psi_c, n_f, n_{tf}$ and projections on planes (ψ_{tf}, ψ_c) and (n_f, n_{tf}) with $\gamma = 2000$ $\gamma_c = 100$.

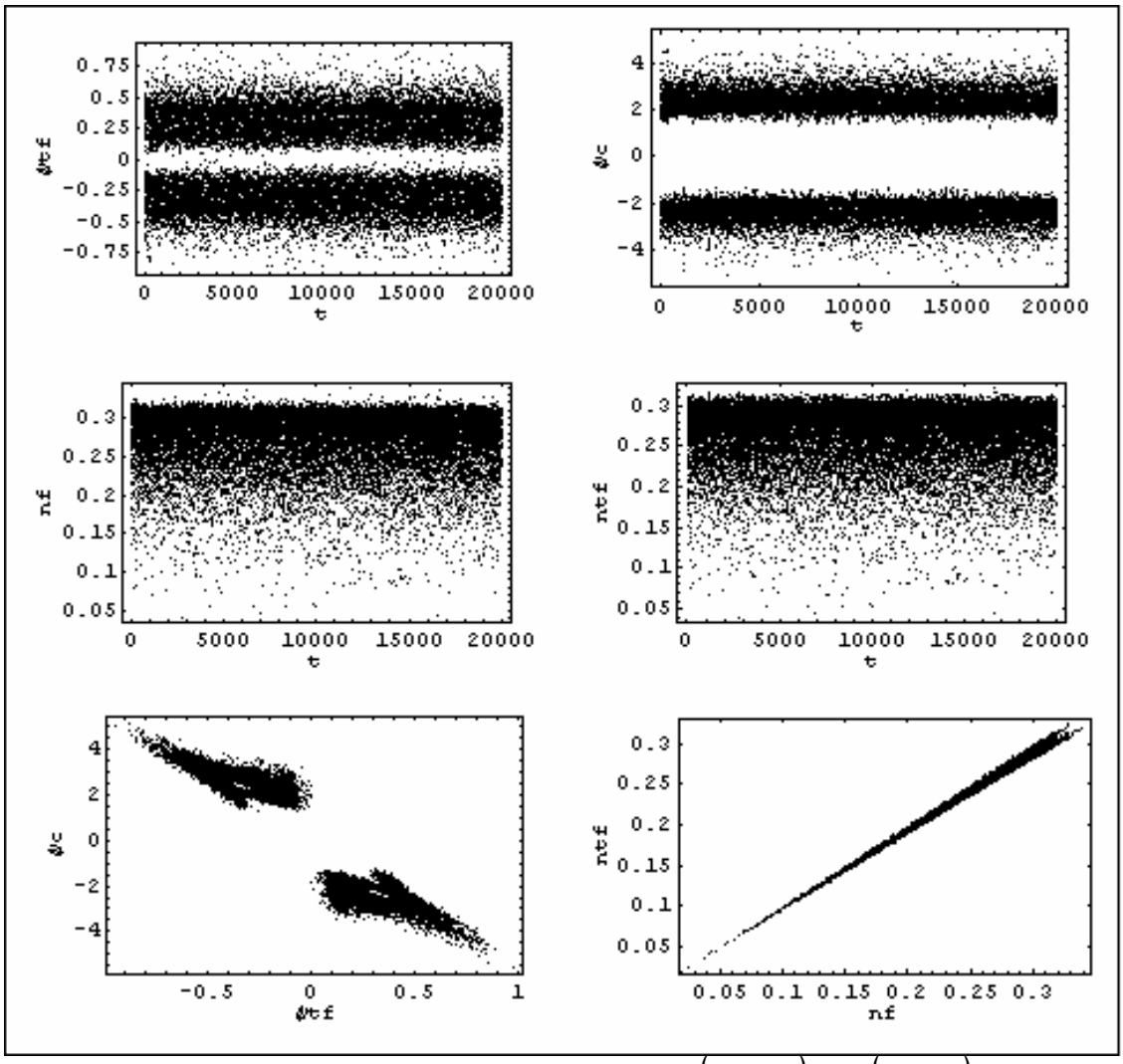

Figure 10: Time series of $\psi_{tc}, \psi_c, n_f, n_{tf}$ and projections on planes (ψ_{tf}, ψ_c) and (n_f, n_{tf}) with $c_{tf} = 0.2$ and $c_c = 0.9$.

4) The market maker cannot affect qualitatively the system dynamics for a wide set of parameter values, in fact, expect for a small periodicity window, the asymptotic dynamics remains chaotic. High values of α (β) decrease (increase) the volume of the attractor.

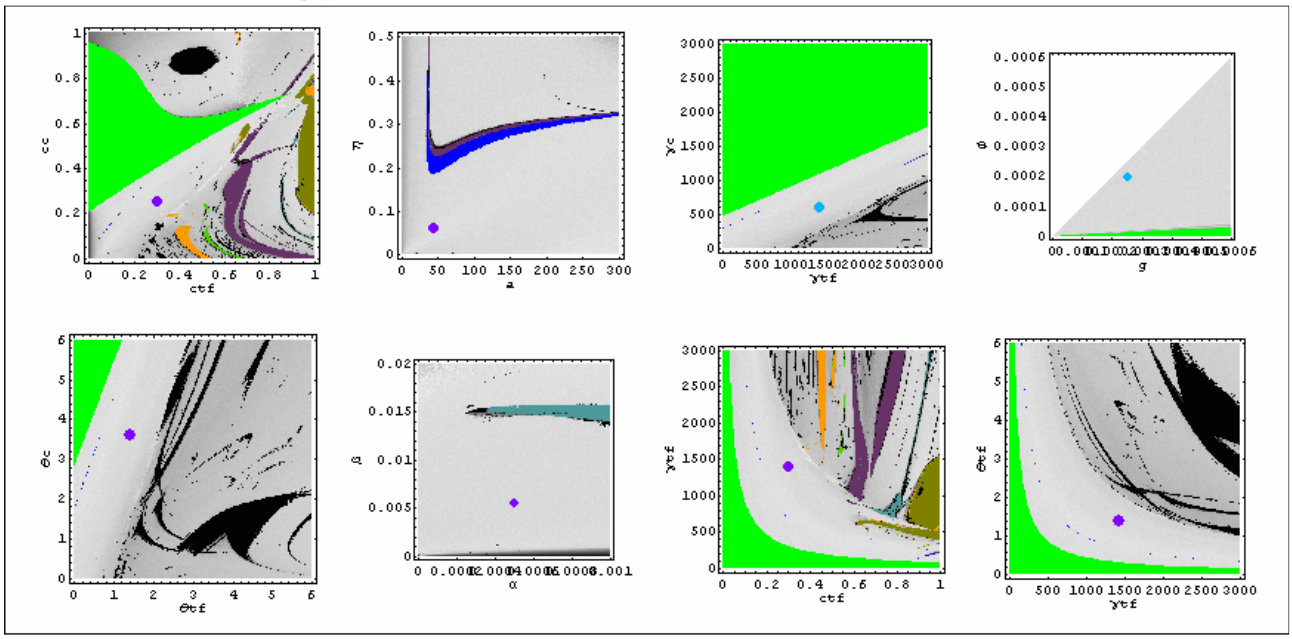

Figure 11: 2-parameter bifurcation diagrams of parameters $(c_{tf}, c_c); (a, \eta); (\gamma_{tf}, \gamma_c); (g, \phi); (\theta_1, \theta_2); (\alpha, \beta); (c_f, \gamma_f); (\gamma_{tf}, \theta_{tf})$ of *System2*. The dots denotes the values of the baseline model.

2.3. Results of stochastic simulations

We have simulated the non-stationary system up to time 30000 adding in each iteration normal incorrelated zero-mean variates to *Equation (7)* and to *Equation (8)* that may be respectively interpreted as noisy trading and random arrival of news. The variances are 0 up to time 20000, in order to let the systems to get sufficiently close to the asymptotic dynamics and subsequently are 0.000025 for the noisy trading and 0.000015 for news information. *Table 3* reports the mean, variance, skewness and kurtosis of the S&P500 index between 1 January 1990 and 31 December 2003 and the mean and variances of the statistics obtained through Monte Carlo simulations of 50 simulated time series. In *Table 4* are reported the mean and variance of the proportions of trend followers, contrarians and mispricing of the simulated series. It is apparent that all strategies survive and are roughly equally balanced and the mispricing averages 1.5. The positive mispricing is due to the fact that the price on the one hand does not diverge from the fundamental in the long run, but on the other does not catch up with an exponentially increasing fundamental. The values of kurtosis and autocorrelation patterns of square returns reported in *Figure 12* denote that the model is able to generate fat tails in the distributions of return and volatility clustering, however the autocorrelation of return is still significant for some time lags. The behaviour of the agents operating in the market outlined in this model is highly stylised in that they can choose between three different strategies but cannot update the strategies through a learning process and does not allow them to profit out of systematic price patterns that would rule out simple autocorrelation at any lag. The model is able to generate time series with a unit-root behaviour as denoted by two sample time series of *System1 and System2* reported in *Figure 13*. The time series generated by *System1* displays larger oscillations in price at high frequencies, because of a high switching speed, this in turn increase the variance of returns. The switching also induces memory in the time series as denoted by a larger value of square return autocorrelations. Therefore a large value of λ may on the one hand describe turbulent phases of the market, on the other hand may give place to a stable equilibrium and affect the size of its basin of attraction. The simulations have underlined that the a large value of λ is associated to a wide basin of attraction. So the effects of switching may be very different on a global scale than on a local one. The effects on global dynamics of λ depends anyhow on the whole set of parameter values, indeed the bifurcation diagrams of λ of *System1* and *System2,* illustrated in *Figure 14*, looks very different from each other. In fact, in the neighbourhood of the equilibrium, the trend following strategy has the smallest prediction error, therefore a high value of the switching parameter induces a higher proportion of agents to switch to the trend following strategy and, since when the system is close the equilibrium trend followers behave like fundamentalists, the size of the basin of attraction increases. On the other hand, if the system is far from equilibrium a high parameter value may induce a high number of agents to select strategies that cause a further departure from the equilibrium. In *Figure 16-19* are represented the autocorrelograms of simple and square returns for parameter values that give place to different asymptotic dynamics of *System1* , the patterns for *System2* are very similar. The autocorrelation patterns for different parameter values denote that:

1) Changes in parameters may leave the asymptotic dynamics qualitatively unchanged, but change the autocorrelation, that is, the market memory. Even with parameter values that give place to converge toward the equilibrium give place to different autocorrelation patters. Transitional dynamics is therefore relevant for nonlinear stochastic systems.

3) High reaction speeds of market maker determine a quick decay in square return autocorrelations.

4) High period cycles may determine cyclical and erratic autocorrelation patterns.

5) The decays in square return autocorrelations when the system converges to a 2-period cycle may be different is the parameter values are inside or outside the Neimark-Sacker boundary, as with $(c_{tf} = 0.29, c_c = 0.37)$ and $(c_{tf} = 0.115, c_c = 0.5)$.

	Mean	Maximum	Minimum	Variance	Skewness	Kurtosis
S&P 500	0.000375309	0.0573148	-0.0686674	0.000110923	-0.0163294	6.49388
System 1	0.00019482	0.300008	-0.1809	0.0291595	0.792829	7.03811
System 2	0.00020626	0.0830494	-0.0789404	0.00020626	-0.0152987	5.76908

Table 3: Statistical properties of S&P 500 and model-generated time series of *System1* and *System2*.

	n_f		n_{tf}		M	
	Mean	**Variance**	**Mean**	**Variance**	**Mean**	Variance
System 1	0.276283	0.077107	0.276283	0.077107	1.50303	0.0733081
System 2	0.33375	0.00327629	0.326909	0.00442164	1.52581	0.0670808

Table 4: Mean and Variance of proportion of fundamentalists, trend followers and mispricing.

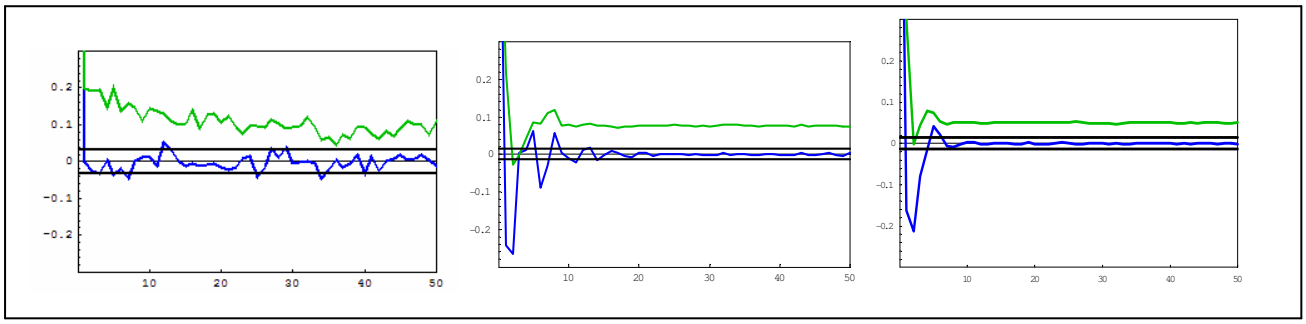

Figure 12: Autocorrelations of returns (blue) and square returns (green) of S&P500 (left panel), *System1* (middle panel) and *System2* (right panel) up to fifty lags.

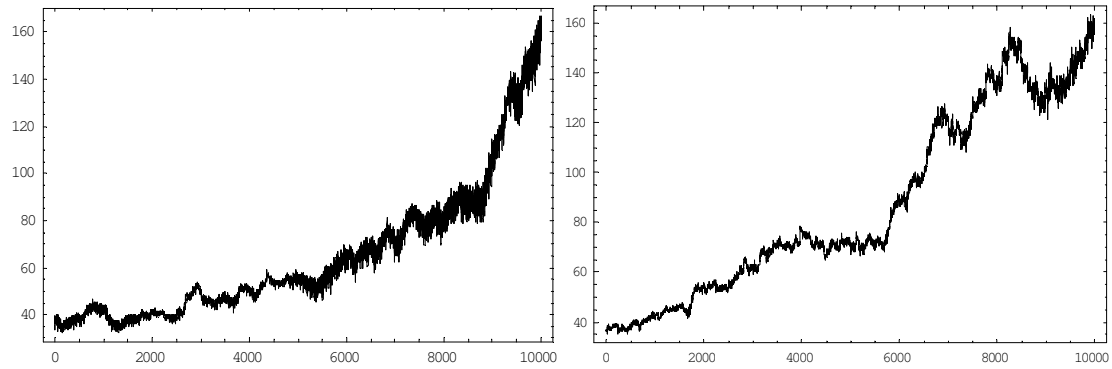

Figure 13: Sample time series of *System1* and *System2*.

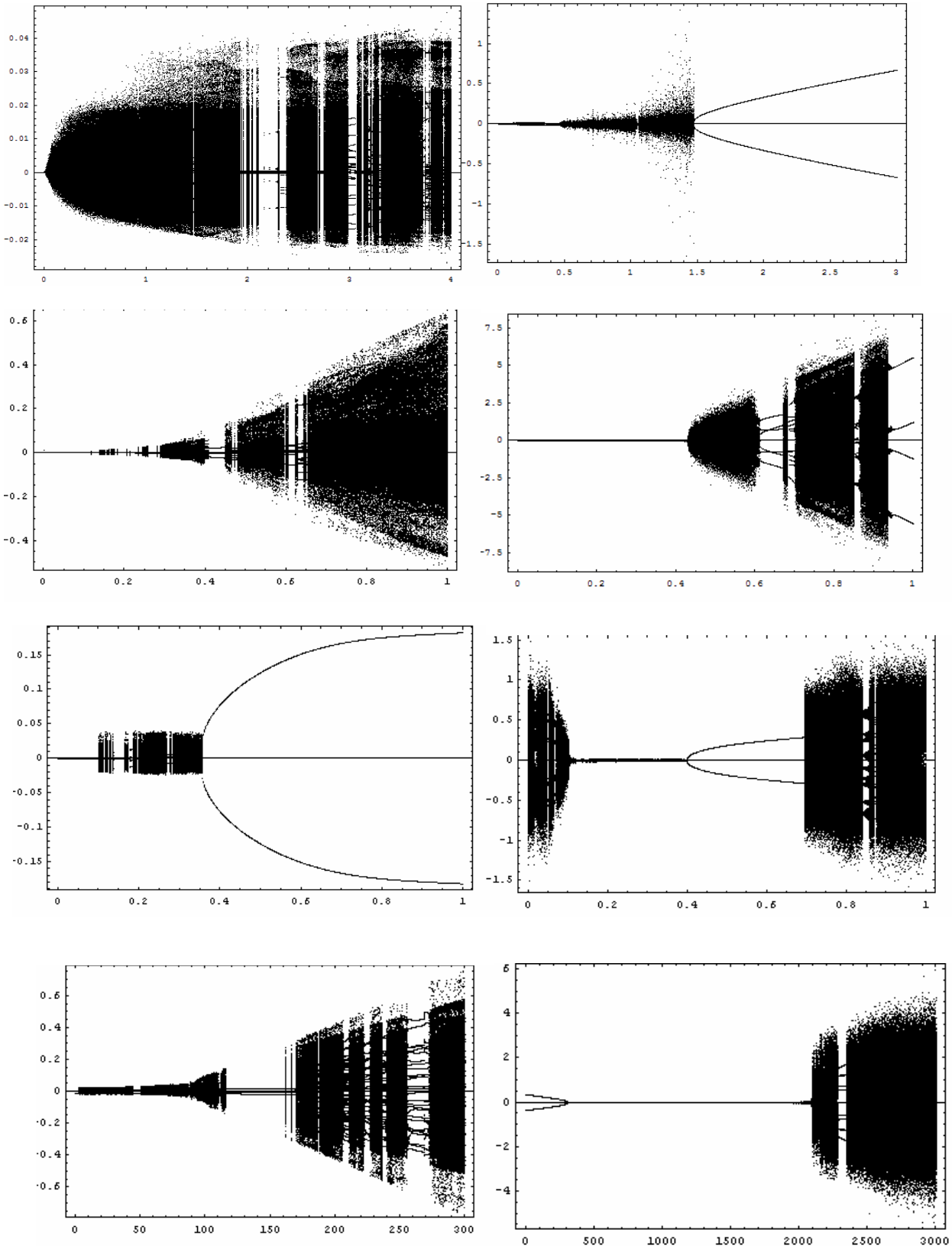

Figure 14:1-parameter bifurcation diagram of $\lambda, c_{tf}, c_c, \gamma_{tf}$ for *System1* (left) and *System2* (right).

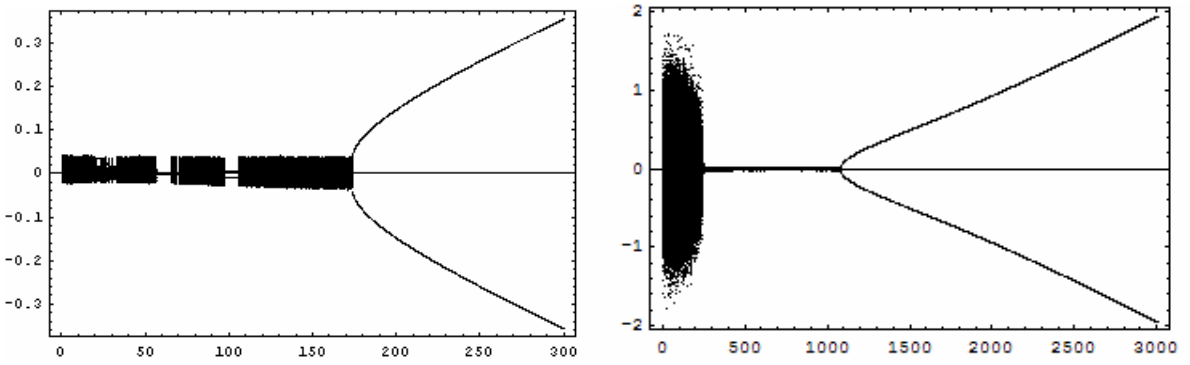

Figure 15:1-parameter bifurcation diagram of γ_c for *System1* (left) and *System2* (right).

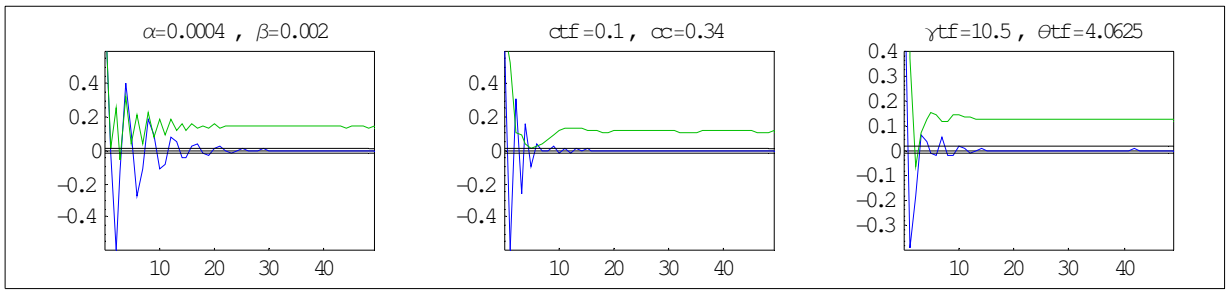

Figure 16:Autocorrelations of returns (blue) and square returns (green) when *System1* converges to the equilibrium.

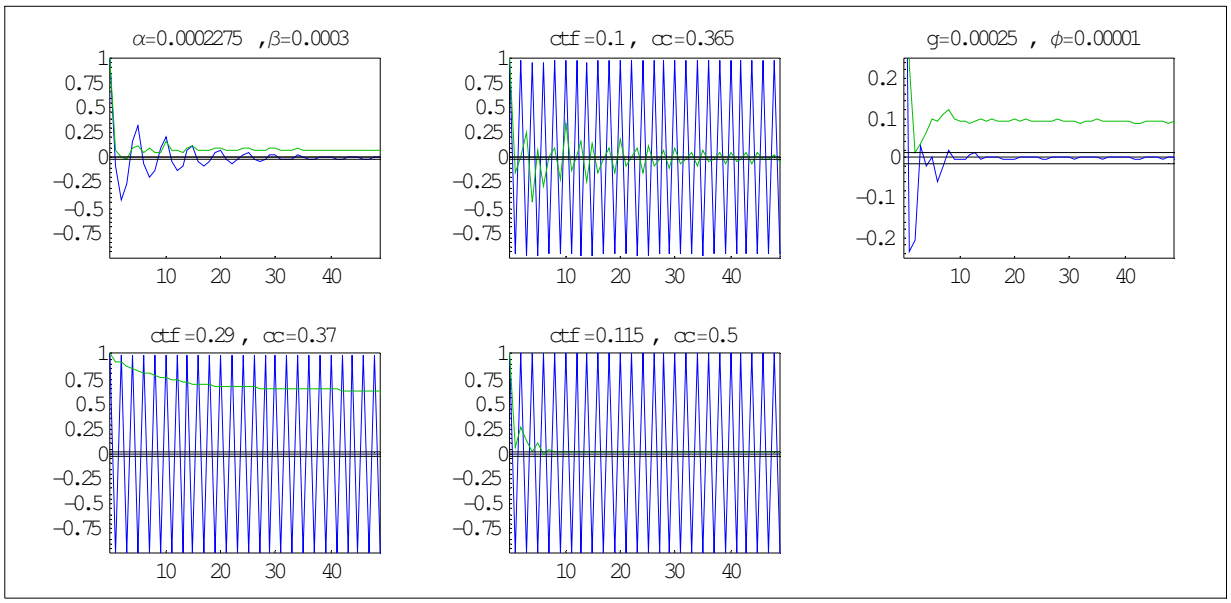

Figure 17:Autocorrelations of returns (blue) and square returns (green) when *System1* converges to 2-period cycles.

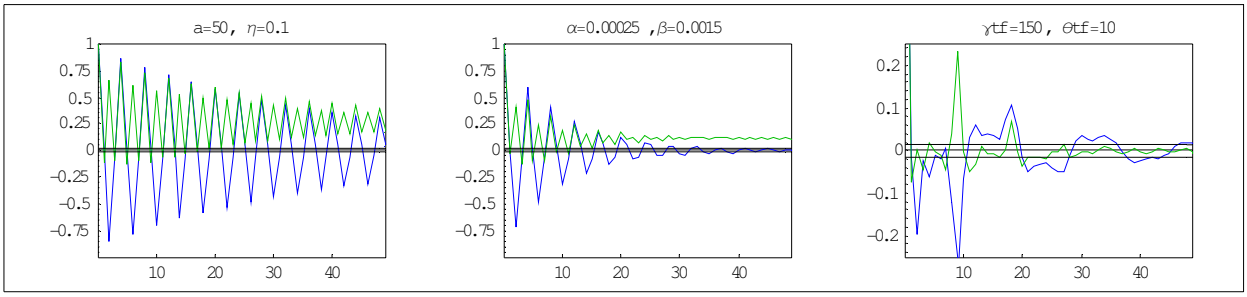

Figure 18:Autocorrelations of returns (blue) and square returns (green) when *System1* converges respectively to cycles of period 4,3 and 5.

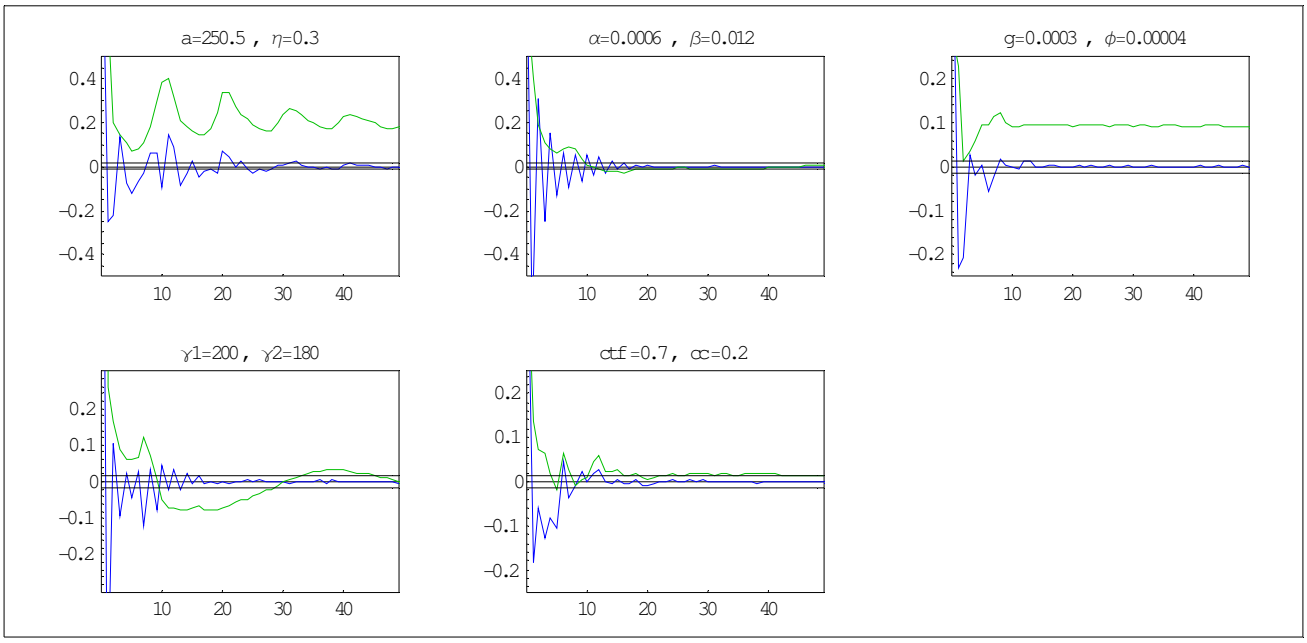

Figure 19:Autocorrelations of returns (blue) and square returns (green) when *System1* converges to strange attractors.

3. The Dynamics of Price and Fundamental Value in a Market with Heterogeneous Strategies and Positive Share Supply

3.1. The model

We will generalize the model by considering now a financial market where one risky and one riskless asset are traded, composed of homogeneous investors who allocate their wealth across fundamentalist, trend following and contrarian strategies and maximize a CRRA utility function defined in terms of wealth. Following Chiarella, Dieci, Gardini (2006), each agent maximize the expected value of the following utility function:

$$\begin{cases} u_i = \dfrac{1}{1-\delta_i}\left(W_i^{1-\delta_i} - 1\right); \delta_i \neq 1 \\ \log(x); \delta_i = 1 \end{cases} \tag{1}$$

Following the same notation of previous chapter, and defining *m* as the logarithm of the dividend-price ratio, the solution to the maximization of (1) with respect to *W* imply that the fraction of wealth invested in the risky asset is approximated by:

$$z_i = \frac{E_i\left[P_t - P_{t-1} + \exp[m] - g\right]}{\delta_i \sigma_i^2\left[P_t - P_{t-1} + \exp[m] - g\right]} \tag{2}$$

Where *m* is the log-dividend yield D_t/P_{t-1}. As proved in Chiarella and He (2001). Chiarella, Dieci, Gardini (2006) prove that the fundamental values would evolve according to the following difference equation:

$$F_t = \phi + F_{t-1} + Log\left[\frac{r_{t-1} - \phi}{r_t - \phi}\right] \tag{3}$$

Where ϕ is the growth rate of the dividends, which are assume to grow exponentially at constant rate and r is a discount rate defined by:

$$r_t = g + Q\left[\frac{1}{\delta_f \sigma_f^2\left(P_t - P_{t-1}\right)} + \frac{1}{\delta_{tf} \sigma_{tf}^2\left(P_t - P_{t-1}\right)} + \frac{1}{\delta_c \sigma_c^2\left(P_t - P_{t-1}\right)}\right] \tag{4}$$

Q is defined as the value of the outstand shares as a fraction of total wealth. We will assume that *W* is constant, that is new stock issue is a fixed proportion of the variation of wealth. We also assume that the fundamental is not know exactly but that agents update the expected fundamental value according to the following process:

$$F_t^E = (1 - c_f) F_t^E + c_f F_t \tag{5}$$

Let us define now the expected mispricing $M_t^E = F_t^E - P_t$ and the change in expected fundamental $\Delta F_t^E = F_t^E - F_{t-1}^E$. The stationary system is given by the following equations:

$$
\begin{aligned}
&\psi_{tf,t,t-1} = (1-c_{tf})\psi_{tf,t-1,t-2} + c_{tf}\rho_t;\ c_{tf} \in (0,1)\\
&\psi_{c,t,t-1} = (1-c_c)\psi_{c,t-1,t-2} - c_c\rho_t;\ c_c \in (0,1)\\
&\Delta F_t^E = (1-c_f)\Delta F_{t-1}^E + c_f\left(\phi + \log\left[\frac{r_{t-2}-\phi}{r_{t-1}-\phi}\right]\right)\\
&M_t = M_{t-1} + \left(\phi + \log\left[\frac{r_{t-2}-\phi}{r_{t-1}-\phi}\right]\right) - \rho_t \qquad (6)\\
&M_t^E = M_{t-1}^E + \Delta F_t^E - \rho_t\\
&n_{i,t} = \frac{\exp\left[-\lambda\log\left[(\rho_t - E_{i,t,t-1})^2\right]\right]}{\sum_j \exp\left[-\lambda og\left[(\rho_t - E_{j,t,t-1})^2\right]\right]}\\
&m_t = m_{t-1} + \phi - \rho_t
\end{aligned}
$$

$$
\begin{aligned}
\xi_t = {} & n_{f,t-1}a\left[M_{t-1} - \frac{g}{\eta}\right] + n_{tf,t-1}\gamma_{tf}\arctan\left[\theta_{tf}\left(\psi_{tf,t-1} - g\right)\right] + n_{c,t-1}\gamma_c\arctan\left[\theta_c\left(\psi_{c,t-1} - g\right)\right] -\\
& \left(n_{f,t-2}a\left[M_{t-2} - \frac{g}{\eta}\right] + n_{tf,t-2}\gamma_{tf}\arctan\left[\theta_{tf}\left(\psi_{tf,t-2} - g\right)\right] + n_{c,t-2}\gamma_c\arctan\left[\theta_c\left(\psi_{c,t-2} - g\right)\right]\right)
\end{aligned}
$$

$$
r_t = g + Q/\left[\frac{n_f a}{\eta} + \frac{n_{tf}\gamma_{tf}\arctan\left[\theta_{tf}\left(\psi_t^{tf} + \exp[m_t] - g\right)\right]}{\left(\psi_t^{tf} + \exp[m_t] - g\right)} + \frac{(1-n_f-n_{tf})\gamma_{tf}\arctan\left[\theta_c\left(\psi_t^c + \exp[m_t] - g\right)\right]}{\left(\psi_t^c + \exp[m_t] - g\right)}\right]
$$

$$
\rho_t = \beta\xi_t + \alpha M_{t-1}^E
$$

The system is characterised by ∞^2 equilibria, indeed every element of the plane (M, δ) is a fixed point of System (6), as the following proposition shows:

Proposition 1. The system has ∞^2 fixed point such as $\psi_{tf} = \phi = \Delta F^E = -\psi_c$, $M^E = \phi/\alpha$, $n_f = n_c = 0; n_{tf} = 1$. Every value of the dividend-price ratio *m* and the actual mispricing *M* are compatible with the fixed point.

Proof. The proof parallels that of *Proposition 1* of the previous chapter, furthermore It can be easily proved that the Jacobian of (6) has two eigenvalue equal to 1, the proof parallel that of previous chapter concerning stability. Therefore the stability cannot be studied by linearization.

3.2. Numerical simulations

As in previous chapter we performed a Monte Carlo simulation by iterating the system up to time 30000 adding in each iteration normal incorrelated zero-mean variates to the equations governing the dynamics of the return and mispricing with variances equal to 0 up to time 20000, in order to let the systems to get sufficiently close to the asymptotic dynamics and subsequently are 0.000025 for the noisy trading and 0.000015 for news information. The parameter and initial values are reported in *Tables (1)* and *(2)*. *Tables (3), (4)* and *(5)* report the statistical results of numerical simulations. *Figure (1)* displays a sample time series of mispricing (left panel) and price (right panel). *Figure (2)* and *(3)* display respectively the autocorrelation of returns and square returns and 2-dimensions bifurcation diagrams.

The results of simulation can be summarised in the following points:

1) the introduction of uncertainty in fundamental value and positive share supply does not affect the statistical results much.

2) Mispricing is characterised by high variance at high frequencies with long period trends even with a learing speed quite high (0.1 percent daily).

3) Estimated mispricing match on average the actual mispricing, but is characterised by a lower volatility because of learning lags.

4) The discount rate is much higher than the risk-free rate (roughly double on annual basis) and the variance is very high. This induces a high volatility in the fundamental value, therefore price volatility may be explained also by rapid changes in the fundamental due not to the arrival of news, but to variations in risk preference and conditional variances. Price volatility is therefore endogenouosly generated by market activity. The variations in discount rate contributes to explaining the phenomenon denoted as Equity Premium Puzzle, because phase characterised by high discount rate are associated to high expected return and high conditional variance estimated by technical traders.

5) Price tends to have high-frequencies oscillations with less volatility than in a model without positive share supply and learning.

6) Fundamentalists may perform a stabilizing action if they believe that price will revert to fundamental quickly, however this depends strongly on initial conditions due to the Cantor structure of the $(a-\eta)$ parameter space and illustrated in *Figure 4*.

7) Price divergence is less likely to occur unless with a high reaction speed of market marker.

	α	β	g	γ_{tf}	γ_{tc}	θ_{tf}	θ_c	c_{tf}	c_c	a	c_f	η	ϕ	λ	Q
	0.0005	0.002	0.00025	1000	1000	1.6	1.6	0.3	0.2	46	0.1	0.006	0.0002	1.4	0.4

Table 1:parameters values.

	$\psi_{tf}(0)$	$\psi_c(0)$	$Z_{tf}(0)$	$Z_c(0)$	n_f	n_{tf}	v_f	v_c	m
	0.01	0	0	0	0	1/3	0	1/3	-9.2101

Table 2: initial values of system variables in numerical simulations.

	Mean	**Maximum**	**Minimum**	**Variance**	**Skewness**	**Kurtosis**
	0.00020018	0.0927566	-0.0629338	0.000223983	0.106366	4.27953

Table 3: Statistical properties of Monte Carlo Simulations.

	n_f		n_{tf}		M	
	Mean	**Variance**	**Mean**	**Variance**	**Mean**	**Variance**
	0.306485	0.062967	0.305589	0.0857697	1.61962	0.897962

Table 4: Mean and Variance of proportion of fundamentalists, trend followers and mispricing.

	M^E		r	
	Mean	**Variance**	**Mean**	Variance
	1.50438	0.309615	0.00038863	0.561815

Table 5: Mean and Variance of expected mispricing and discount rate.

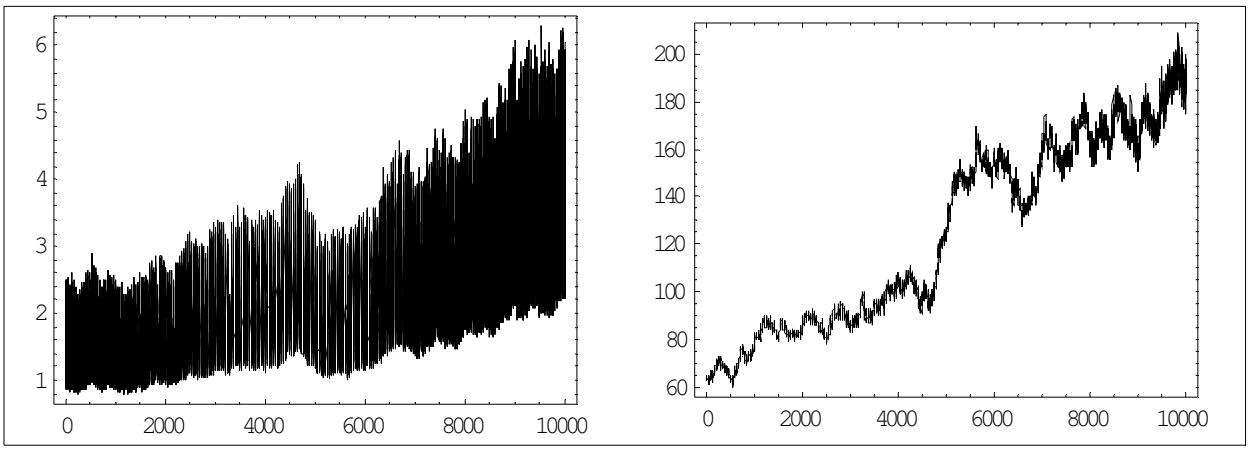

Figure 1: Sample time series of mispricing and price.

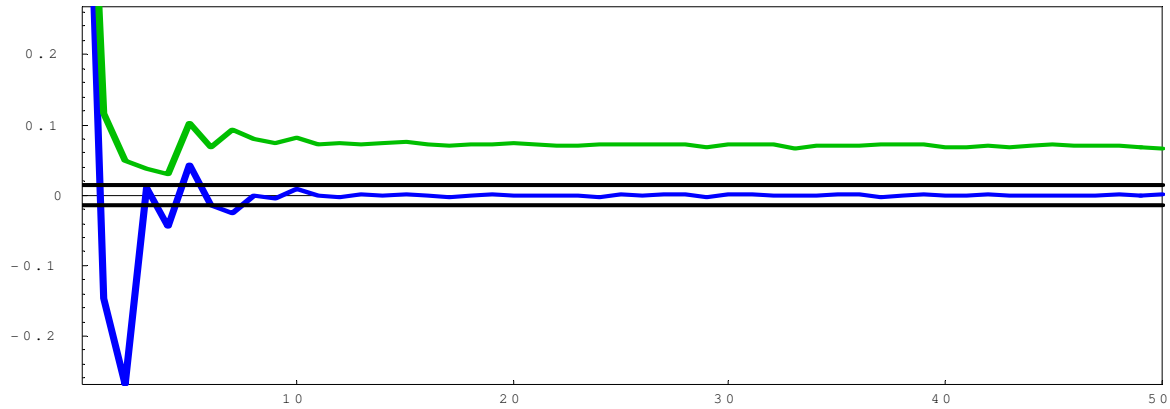

Figure 2: Autocorrelations of returns (blue) and square returns (green) up to fifty lags.

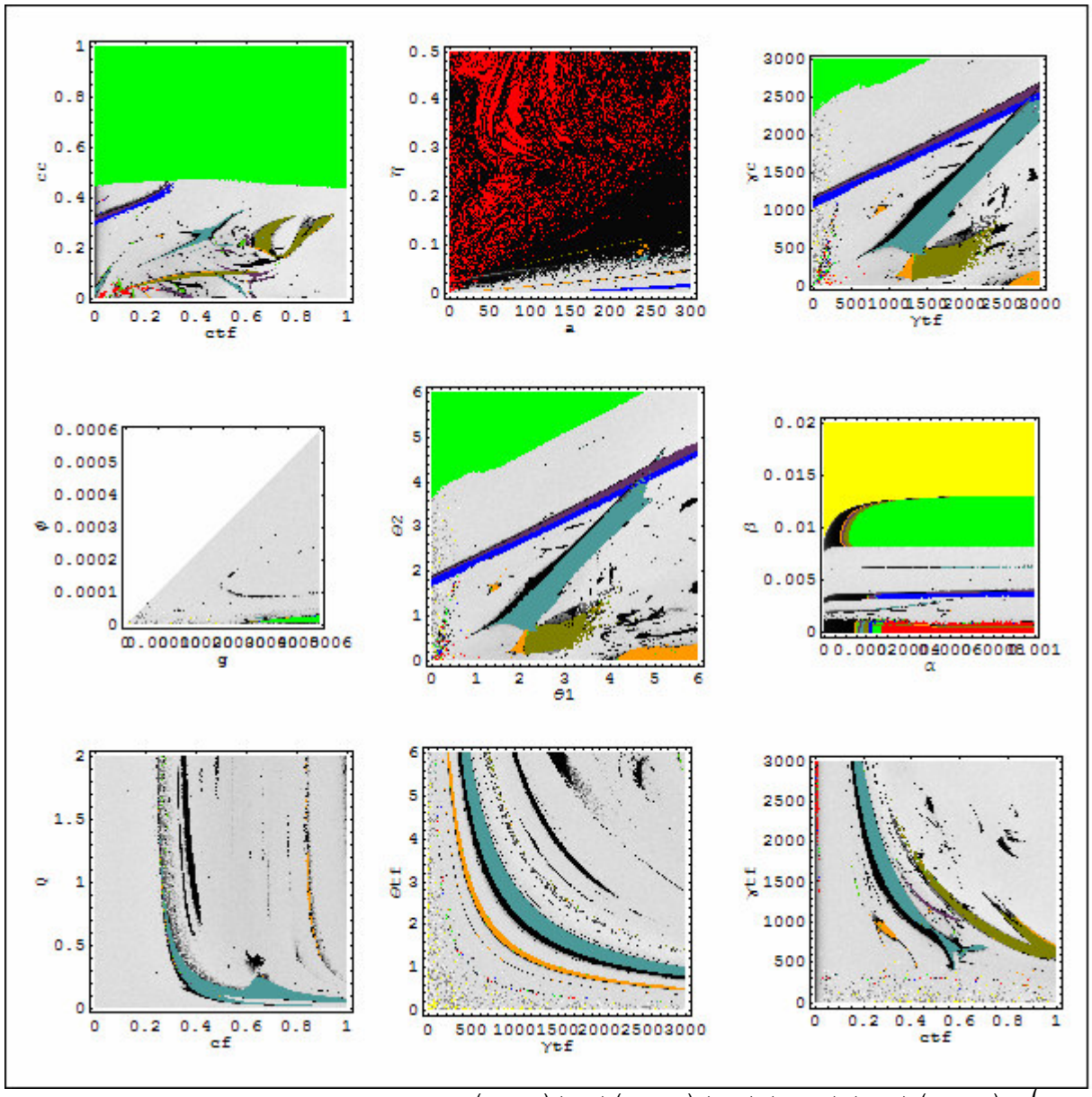

Figure 3: 2-dimensional bifurcation diagrams $(c_{tf}, c_c);(a,\eta);(\gamma_{tf}, \gamma_c);(g,\phi);(\theta_1,\theta_2);(\alpha,\beta);(c_f,\gamma_f);\ (\gamma_{tf},\theta_{tf});$ (c_{tf},γ_{tf}).

.

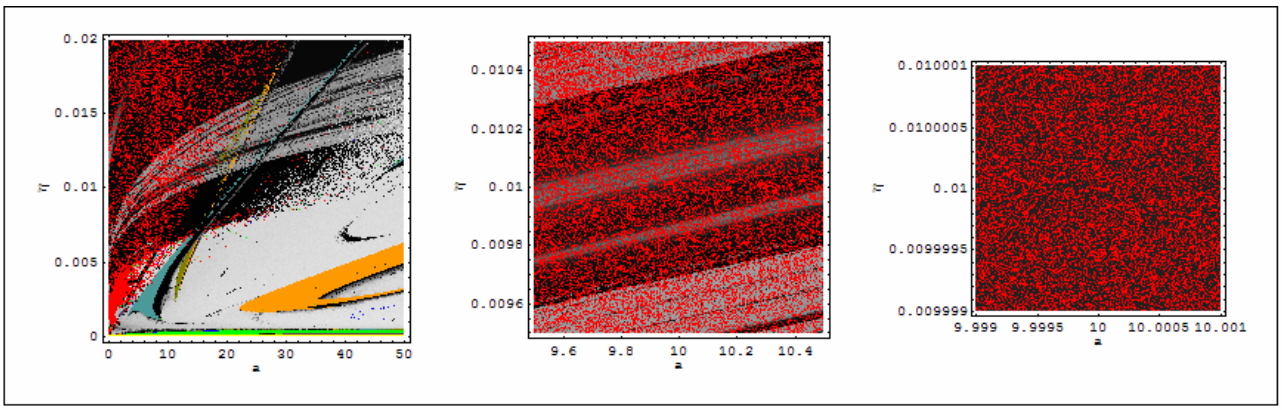

Figure 4: magnification of (a,η) bifurcation diagram.

Conclusion

We have outlined continuous and discrete time models of a financial market with heterogeneous interacting agents. The dynamical systems shows periodic, quasi-periodic and strange attractors, and are able to generate some stylized facts present in real markets, even in a purely deterministic setting: excess kurtosis, volatility clustering and long memory. We have indeed tuned the parameters in order to produce artificial time series with statistical properties similar to those of the daily time series of S&P500 index between 1 January 1990 and 31 December 2003. Mean, variance and kurtosis tend to match quite close those of the S&P500, whereas skewness and autocorrelation patterns are somewhat affected by the long run exponentially increasing fundamental value and price. The model analysed in chapter 1, while unable to completely cancel the autocorrelations of returns and to give rise to square autocorrelations that decay according to a power law, allows for a reduction in the autocorrelation with respect to TDG, which is characterized only by fundamentalist agents and shows a very high negative first order autocorrelation, because fundamentalists tend to drive the price back to fundamental too quickly. Even in the case where fundamentalists are the only agents present in the market, they are unable to drive the price back to the fundamental on a steady state trajectory, because of both the increasing risk aversion as they trade in order to profit out of a mispricing and the delays in processing the information from the market. Moreover, the increase in the fundamentalist reaction speed on the one hand may destroy the strange attractor giving rise to a chaotic transient, on the other may even increase the disorder in the system, as pointed out by the values of the Lyapunov exponent, because the fundamentalists trigger a strong response of technical traders. It may also be possible that, when the fraction of fundamentalists is low, trend followers and contrarians give rise to synchronization in the system, bringing about a dramatic change in the dynamics. In this case, the system exhibits the phenomenon of intermittency, that is, regular phase interrupted by chaotic bursts in the dynamics. The introduction of an evolutionary switching between technical traders leads to an increase in the volatility and in the kurtosis, provided that the speed of switching is not too high because otherwise the increase in the variance makes it less likely that returns will fall in the tails of the distributions. The models described in chapter 2 and 3 following the standard paradigm of utility maximization, but, differently from most of the literature on interacting agents, utilize a flow-based approach where excess demand is determined by the difference between optimal and current holdings of the asset and consider a realistic values for the interest rate and the growth rate. We have proved that a high value of the swithching speed while, on the hand, stabilizes the system locally, on the other give rise to high-frequency high-volatility oscillations and price divergence in some cases. The local stability is determined by the reaction speed of trend followers and the market maker, but the behavior of the other investors affect the global dynamics. Those models confirm that fundamentalists are not able to stabilize the market, unless they are not fully informed on the fundamental and believe that price is strongly reverting about the fundamental. Even in this case the final outcome is uncertain because of coexistence of attractors and Cantor structure of the parameter space. There are many ways to extend the models. While in the present paper the switching and reaction speeds are constant, an extension will render them state-dependent. Another extension will consider time delays distributed according to distributions that give more importance to more recent observations as well as technical traders who take into account the whole history of past prices. Such extensions should produce time series with long run chaotic dynamics displaying more realistic statistical properties, mainly in terms of autocorrelation patterns and long memory.

References

Beja, A. and Goldman, M. (1980), *On the dynamic behavior of prices in disequilibrium,* Journal of Finance **35**, 235-247.

Brock, W. A. (1997), *Asset price behavior in complex environment*, in: Arthur, W. B., Durlauf, S. N. and Lane D.A., eds., The Economy as an Evolving Complex System II, Addison-Wesley, Reading, MA, 385-423.

Brock, W. A., Hommes C. H. (1997), *A rational route to randomness*, Econometrica **65**, 1059-1095.

Brock, W.A. and Hommes, C. H. (1998), *Heterogeneous beliefs and routes to chaos in a simple asset pricing model*, Journal of Economic Dynamics and Control **22**, 1235-1274.

Brock, W.A. and Hommes, C. H. (2001), *Heterogeneous beliefs and routes to complex dynamics in asset pricing models with price contingent contracts*, Working Paper, CeNDEF, University of Amsterdam.

Brock, W. A., Hommes C. H., Wagener, F. O. O. (2005), *Evolutionary dynamics in markets with many traders type*, Journal of Mathematical Economics **41**, 7-42.

Caginalp, G. and Ermentrout G. B. (1990), *A kinetic thermodynamics approach to psychology of fluctuations in financial markets*, Applied Mathematics Letters **3**, 17-19.

Caginalp, G. and Ermentrout G. B. (1991), *Numerical studies of differential equations related to theoretical financial markets*, Applied Mathematics Letters **4**, 35-38.

Chiarella, C. (1992), *The dynamics of speculative behaviour*, Annals of Operations Research **37**, 101-123.

Chiarella, C., Dieci, R. and Gardini L. (2002), *Speculative behaviour and complex asset price dynamics: a global analysis*, Journal of Economic Behaviour and Organization **49**, 173-197.

Chiarella, C., Dieci, R. and Gardini L. (2005), *The dynamics interaction of speculation and diversification*, Applied Mathematical Finance **12**, 17-52.

Chiarella, C., Dieci, R. and Gardini L. (2005), *The dynamics interaction of speculation and diversification*, Applied Mathematical Finance **12**, 17-52.

Chiarella, C. and He, X.-Z. (2001), *Asset pricing and wealth dynamics under heterogeneous expectations*, Quantitative Finance **1**, 509-526.

Chiarella, C. and He, X.-Z. (2002), *Heterogeneous beliefs, risk and learning in a simple asset pricing model*, Computational Economics **19**, 95-132.

Chiarella, C. and He, X.-Z. (2006), *Asset price and wealth dynamics in a financial market with heterogeneous agents*, Journal of Economic Dynamics and Control, 30, 9-10, 1755-1786, 2006.

Day, R. and Huang, W. (1990), *Bulls, bears and market sheep*, Journal of Economic Behavior and Organization **14**, 299-329.

Franke R. and Sethi R. (1998), *Cautious trend-seeking and complex asset price dynamics*, Research in Economics **52**, 61-79.

Gaunersdorfer, A. (2000), *Endogenous fluctuations in a simple asset pricing model with heterogeneous agents*, Journal of Economic Dynamics and Control **24**, 799-831.

Gaunersdorfers, A. and Hommes, C.H. Wagener, F. (2000), *Bifuraction routes to volatility clustering*, Working Papers SFB "Adaptive Information Systems and Modelling in Economics and Management Science", Nr. 73.

Gaunersdorfers, A. and Hommes, C.H. (2005), *A nonlinear structural model for volatility clustering*, in: Teyssière G. and Kirman A., eds., Long Memory in Economics, Spring-Verlag, forthcoming.

Grebogi C., Ott E. and Yorke J. A. (1986), *Critical exponent of chaotic transients in nonlinear dynamical systems*, Physical Review Letters **57**, 1284-1287.

Grebogi C., Ott E., Romeiras F. and Yorke J. A. (1987), *Critical exponent for crisis-induced intermittency*, Physical Review A **36**, 5365-5380.

He, X.-Z. (2003), *Asset pricing, volatility and market behavior: a market fraction approach*, Working paper, Research Papers Series **95**, Quantitative Finance Research Centre, University of Technology, Sydney.

Hoover, W.G. (1985), *Canonical dynamics: equilibrium phase-space distributions*, Physical Review A **31**, 1695-1697.

Levy, M., Levy, H. (1996), *The danger of assuming homogeneous expectations*, Financial Analysts Journal **52**, 65-70.

Mandelbrot, B. B., Fisher, A. and Calvet, L. (1997), *A multifractal model of asset returns*, Working paper, Cowles Foundation Research Paper **1164**, Yale University.

Nosè, S. (1984a), *A unified formulation of the constant temperature molecular dynamics method*, The Journal of Chemical Physics **81**, 511-519.

Nosè, S. (1984b), *A molecular dynamics method for simulation in the canonical ensemble*, Molecular Physics **52**, 255-268.

Nosè, S. (1991), *Molecular dynamics simulations,* Progress of Theoretical Physics Supplement **103**, 1-49.

Sethi, R. (1996), *Endogenous regime switching in speculative markets*, Structural Change and Economic Dynamics **7**, 99-118.

Sonis, M. (2000), *Critical bifurcation surfaces of 3D discrete dynamics*, Discrete Dynamics in Nature and Society 4, 333.343.

Thurner, S., Dockner, E.J., Gaunersdorfer, A. (2002), *Asset Price Dynamics in a model of investors operating on different time horizons*, Working paper, University of Vienna.

Westerhoff, F. (2003), *Bubbles and crashes: optimism, trend extrapolation and panic*, International Journal of Theoretical and Applied Finance **6**, 829-833.

Westerhoff, F. (2004a), *Greed, fear and stock market dynamics*, Physica A: Statistical Mechanics and its Application **343C**, 635-642.

Westerhoff, F. (2004b), *Market depth and price dynamics: a note*, International Journal of Modern Physics C **15**, 1005-1012.